

---

# Optimal Design for Adaptive In-Context Prompt Tuning in Large Language Models

---

<b>Subhojyoti Mukherjee*</b> ECE Department UW-Madison Wisconsin, Madison smukherjee27@wisc.edu	Anusha Lalitha AWS AI Labs Santa Clara USA	Aniket Deshmukh AWS AI Labs Santa Clara USA	Ge Liu AWS AI Labs Santa Clara USA
	Yifei Ma AWS AI Labs Santa Clara USA	Branislav Kveton AWS AI Labs Santa Clara USA	

## Abstract

One emergent ability of large language models (LLMs) is that query-specific examples can be included in the prompt at inference time. In this work, we use active learning for adaptive prompt design and call it **Active In-context Prompt Design (AIPD)**. We design the **LLM** prompt by adaptively choosing few-shot examples from a training set to optimize performance on a test set. The training examples are initially unlabeled and we obtain the label of the most informative ones, which maximally reduces uncertainty in the **LLM** prediction. We propose two algorithms, **GO** and **SAL**, which differ in how the few-shot examples are chosen. We analyze these algorithms in linear models: first **GO** and then use its equivalence with **SAL**. We experiment with many different tasks in small, medium-sized, and large language models; and show that **GO** and **SAL** outperform other methods for choosing few-shot examples in the **LLM** prompt at inference time.

## 1 Introduction

Large language models (LLMs), such as Vicuna [Chiang et al., 2023], Falcon-40B [Penedo et al., 2023], and OpenLLaMA [Touvron et al., 2023] are applied in mainly two ways: fine-tuning and prompt tuning. In fine-tuning, the **LLM** weights are adapted to a downstream task [Devlin et al., 2018]. Fine-tuning can easily incorporate domain knowledge that a pre-trained model may not possess and resembles classic inductive inference. Fine-tuned models often do not need carefully designed prompts, which makes them easier to deploy. The main drawback of fine-tuning is that it can be costly, because tens of thousands of training examples may be needed to fine-tune billions of parameters of the **LLM** [Ding et al., 2023]. In prompt tuning, the **LLM** weights are fixed and the **LLM** is given query-specific examples at inference time that affect its output [Lester et al., 2021]. This ability to conduct in-context inference is one of the emergent abilities of **LLMs**. Prompt tuning does not require large training sets. It is also preferred when query-specific examples are private or change over time, and thus can only be utilized at inference time.

Prior works on prompt tuning mainly focus on hard prompts, which are carefully handcrafted to get the desired output. This can be time-consuming and fragile, as minor prompt modifications can

---

\*Work conducted during an internship at Amazon.

lead to a significant performance drop on the downstream task [Suzgun et al., 2022]. In contrast, Zhang et al. [2022a,b] and Diao et al. [2023] explored adaptive prompt design using clustering-based and uncertainty-reducing approaches. While these approaches offer some benefits, we argue that optimal designs [Pukelsheim, 2006, Fedorov, 2013] can outperform them by effectively balancing uncertainty and diversity. Similarly to Zhang et al. [2022a,b] and Diao et al. [2023], we propose a framework for adaptive prompt design called *active in-context prompt design (AIPD)*. The key idea is to design the LLM prompt by adaptively choosing few-shot examples for a set of test examples at inference time. The examples are initially unlabeled and we obtain labels for the most informative ones, which maximally reduce the uncertainty in the LLM prediction for all test examples. We assume that the observed labels are collected from experts (human-in-the-loop) or revealed by an oracle [Dasgupta, 2005, Hanneke et al., 2014]. The focus on informativeness and diversity ensures efficient label acquisition by selecting the best examples. This reduces reliance on limited and costly resources such as expert labeling.

One motivating example for our work is *theme recognition*, where the goal is to identify a unifying theme for a set of items (e.g., movies, grocery items, or books) provided by the user. For example, let the test query be a triplet of movie titles “Lion King”, “Jungle Book”, and “Tarzan”, and the goal is that the LLM should infer a plausible common theme such as “Disney animated movies”, “Children’s movies”, or “Movies with deep connections with nature”. This task is challenging due to the inherent ambiguity and many plausible themes. To address this, we can give the LLM a few informative examples of triplets of movies and their common themes as training examples in context that can guide it towards the correct theme for the test query. This inherently requires a human-in-the-loop who can go over the set of triplets of movies and label their common theme for each example which can be costly. Hence, it is critical to narrow down to a few informative examples from exponentially many training examples possible for vast amounts of data like movies. Finally note that by exposing the LLM to these training examples, we refine its understanding of the task, improve handling of ambiguity, and thus improve its ability to identify the common theme for unseen test examples. To address the above challenges, we propose a framework for adaptive prompt design called active in-context prompt design (AIPD). Our framework is general and can be easily extended to any active supervised-learning task, like active regression [Gao and Koller, 2011] and active classification [Gao and Koller, 2011]. At a high level, we treat the LLM as a general inference machine [Brown et al., 2020b, Mirchandani et al., 2023] that is shown adaptively-chosen examples with labels at inference time. The LLM then utilizes them to answer any set of related test examples. The key idea is to choose the next example to label such that we maximally reduce the estimated uncertainty of the answer to the test examples. We focus on designing algorithms with the following two properties: (1) Implementable in any LLM that can be queried efficiently. The parameters of the LLM do not change or have to be observed. (2) Analyzable in simple models. In this work, we use linear models to motivate and analyze our algorithms.

We now state the main contributions of our work:

- (1) We propose a **G-Optimal** design algorithm (**GO**). The key idea in **GO** is to retrieve the examples to label that are closest to the set of test examples in the inference task. Our main contribution is the right notion of closeness, based on posterior covariance in a simpler model. **GO** is implementable with any LLM that can be sampled from, and does not require access to model parameters, feature embeddings of the LLM, or its gradients.
- (2) We propose a **Simulation-Based Active Learning** algorithm (**SAL**). **SAL** uses simulation to estimate the impact of labeling unlabeled examples on uncertainty of the example in the inference task. **SAL** is also implementable with any LLM that can be sampled from.
- (3) **GO** is motivated by optimal designs in linear models [Kiefer and Wolfowitz, 1960, Pukelsheim, 2006]. This allows us to analyze **GO** in linear models (Theorem 1). Our proof is a major departure from similar analyses in fixed-budget best-arm identification in bandits [Azizi et al., 2022, Yang and Tan, 2022], for instance because we directly analyze the discrete allocation problem and each unlabeled example can be labeled at most once. We discuss this in detail right after Theorem 1. **SAL** is more general than **GO** because it does not make any linear model assumption in its design. We show that **SAL** and **GO** are equivalent in linear models in Theorem 2.
- (4) We evaluate **GO** and **SAL** on UCI [Markelle Kelly, 1988] and OpenML [Vanschoren et al., 2013] regression and classification tasks, custom NLP datasets, abstract reasoning corpus (ARC) tasks [Alford, 2021, Mirchandani et al., 2023], and Probabilistic Context Free Grammar (PCFG) tasks

[Hupkes et al., 2020]. **GO** and **SAL** consistently outperform other active prompt tuning methods [Zhang et al., 2022a,b, Diao et al., 2023] for choosing few-shot examples in majority of the tasks.

We advance the understanding of active in-context prompt design in **LLMs** and develop a practical methodology for adaptive prompt design. To our knowledge, this is the first paper that analyzes optimal design based prompting approaches that correctly balance uncertainty and diversity-based sampling as opposed to other existing adaptive prompting-based approaches [Zhang et al., 2022a,b, Diao et al., 2023].

This paper is organized as follows. Section 2 introduces the problem setting. Section 3 presents our methods and discusses their properties. Section 4 is devoted to analyzing our methods. Section 5 validates our approach empirically. We review related work in detail in Appendix A. Finally, Section 6 summarizes our contributions and suggests avenues for future work.

## 2 Setting

We pose the problem of adaptive prompt design as active learning. We adopt the following standard active learning terminology [Lewis, 1995, Tong and Koller, 2001, Dasgupta, 2005, Dasgupta et al., 2007, Hanneke et al., 2014]. We have a  $d$ -dimensional *feature space*  $\mathcal{X} \subset \mathbb{R}^d$  and a  $d_y$ -dimensional *label space*  $\mathcal{Y} \subseteq \mathbb{R}^{d_y}$ . A labeled example is a pair  $(\mathbf{x}, Y) \in \mathcal{X} \times \mathcal{Y}$ . The feature vectors and labels are related as  $Y = f(\mathbf{x}, \theta_*) + \varepsilon$ , where  $f$  is an underlying model,  $\theta_*$  is its parameter, and  $\varepsilon$  is an *independent zero-mean noise vector*. Our goal is to learn to estimate  $f$  on test examples by labeling training examples. We have a budget  $T$  on the maximum number of training examples that can be labeled. This constraint can arise due to multiple reasons. For instance, human labels may be necessary and they are naturally costly. Another reason may be that the machine learning model has a limited capacity for including labeled examples, such as the length of prompts in **LLMs** [Zhang et al., 2022a,b, Diao et al., 2023].

Now we introduce our notation in detail. Denote  $[m] = \{1, 2, \dots, m\}$ . We have  $n$  *training examples*  $\mathcal{X}_{\text{examples}} = \{\mathbf{x}_1, \dots, \mathbf{x}_n\}$  and  $K$  *test examples*  $\mathcal{X}_* = \{\mathbf{x}_{*,1}, \dots, \mathbf{x}_{*,K}\}$ . We assume that both sets are related, such as being sampled from the same distribution. The label of the test example  $\mathbf{x}_{*,k}$  is  $Y_{*,k}$ . In our motivating theme recognition example the training examples  $\mathbf{x}_i$  and test example  $\mathbf{x}_{*,k}$  is a concatenation of triplets of movies, and the label  $Y_i$  or  $Y_{*,k}$  is the common theme amongst the triplets respectively. We want to infer  $Y_{*,k}$  for all  $k \in [K]$  without explicitly modeling the complex function  $f$ . We model the function using an **LLM** which we treat as a general inference machine because of its large representation capacity [Brown et al., 2020a, Mirchandani et al., 2023]. Specifically, let  $H_t = \{(X_\ell, Y_\ell)\}_{\ell \in [t-1]}$  be a set of  $t-1$  previously labeled examples, where  $X_\ell \in \mathcal{X}_{\text{examples}}$  is the  $\ell$ -th labeled example and  $Y_\ell$  is its label. Then we denote by  $p(\cdot | \mathbf{x}, H_t)$  the distribution over labels of an **LLM** for a queried example  $\mathbf{x}$  when  $H_t$  is used as few-shot in-context examples. To implement this in the **LLM**, we simply concatenate  $\mathbf{x}$  and  $H_t$  in context [Zhang et al., 2022a,b, Diao et al., 2023]. We know that in-context examples affect the distribution of responses of an **LLM** [Xie et al., 2021, Suzgun et al., 2022, Deng et al., 2023, Lee et al., 2023]. So, the problem of learning  $f$  under a budget  $T$  can be viewed as selecting  $H_{T+1}$  such that  $p(Y_{*,k} | \mathbf{x}_{*,k}, H_{T+1})$  is high for all test examples  $k \in [K]$ . This problem is challenging, especially when the training examples need to be labeled.

To effectively reduce the uncertainty of  $Y_{*,k} | \mathbf{x}_{*,k}, H_{T+1}$ , we need to quantify it. One possibility is to use the entropy  $-\mathbb{E}_{Y_{*,k} \sim p(\cdot | \mathbf{x}_{*,k}, H_{T+1})}[\log p(Y_{*,k} | \mathbf{x}_{*,k}, H_{T+1})]$ . This is problematic because the entropy is hard to estimate for high-dimensional random variables [Vershynin, 2020], especially without having access to  $p(\cdot | \mathbf{x}_{*,k}, H_{T+1})$  beyond sampling from it. This is a shortcoming of recent adaptive prompting techniques [Zhang et al., 2022a,b, Diao et al., 2023]. Therefore, we propose using the covariance of  $Y_{*,k} | \mathbf{x}_{*,k}, H_{T+1}$  as the uncertainty measure. Specifically, we measure the uncertainty of the  $k$ -th test example by  $\text{tr}(\text{cov}[Y_{*,k} | \mathbf{x}_{*,k}, H_{T+1}])$  and the uncertainty over all test examples by  $\max_{k \in [K]} \text{tr}(\text{cov}[Y_{*,k} | \mathbf{x}_{*,k}, H_{T+1}])$ . Since the trace of the covariance is the sum of the variances in individual dimensions, our objective can be interpreted as minimizing the maximum variance over the predicted labels of all test examples. This is a natural measure of uncertainty in linear models and corresponding optimal designs [Pukelsheim, 2006, Fedorov, 2013].

Before we present our algorithms, we wanted to outline their general design. Given a budget  $T$ , we design sequential adaptive algorithms over  $T$  rounds, where the example  $X_t \in \mathcal{X}_{\text{examples}}$  in round  $t \in [T]$  is chosen as a function of  $H_t = \{(X_\ell, Y_\ell)\}_{\ell \in [t-1]}$  up to that round. Since  $H_t$  summarizes past actions of the algorithm, we call it a *history*. The label of example  $X_t$  is  $Y_t = f(X_t, \theta_*) + \varepsilon_t$ ,

---

**Algorithm 1** G-optimal design (GO)

---

- 1: **Input:** Training set  $\mathcal{X}_{\text{examples}} = \{\mathbf{x}_i\}_{i=1}^n$ , test set  $\mathcal{X}_* = \{\mathbf{x}_{*,k}\}_{k=1}^K$ , budget  $T$
  - 2:  $\mathcal{L}_1 \leftarrow \emptyset, \mathcal{U}_1 \leftarrow [n], H_1 \leftarrow \{\}$
  - 3: **for**  $t = 1, \dots, T$  **do**
  - 4:  $I_t = \arg \min_{i \in \mathcal{U}_t} \max_{k \in [K]} \mathbf{x}_{*,k}^\top \left( \widehat{\Sigma}_t^{-1} + \mathbf{x}_i \mathbf{x}_i^\top \right)^{-1} \mathbf{x}_{*,k}$
  - 5:  $X_t \leftarrow \mathbf{x}_{I_t} \in \mathcal{X}_{\text{examples}}$
  - 6: Observe label  $Y_t$  of example  $X_t$
  - 7:  $\mathcal{L}_{t+1} \leftarrow \mathcal{L}_t \cup \{I_t\}, \mathcal{U}_{t+1} \leftarrow \mathcal{U}_t \setminus \{I_t\}$
  - 8:  $H_{t+1} \leftarrow H_t \cup \{(X_t, Y_t)\}$
  - 9: **end for**
  - 10: **Output:** Sample  $Y_{*,k} \sim p(\cdot \mid \mathbf{x}_{*,k}, H_{T+1})$  for  $k \in [K]$
- 

where  $\varepsilon_t$  is an independent zero-mean noise vector in round  $t$ . Our objective is to minimize the maximum uncertainty over all test examples,  $\max_{k \in [K]} \text{tr}(\text{cov}[Y_{*,k} \mid \mathbf{x}_{*,k}, H_{T+1}])$ .

### 3 Algorithms

In this section, we introduce our active learning algorithms for selecting most informative training examples from  $\mathcal{X}_{\text{examples}}$ . To simplify notation, we assume scalar labels and then discuss an extension to vector labels at the end of the section. We also let  $\mathcal{L}_t \subseteq [n]$  and  $\mathcal{U}_t \subseteq [n]$  be the indices of all labeled and unlabeled training examples up to round  $t$ , respectively. Note that  $\mathcal{L}_t \cup \mathcal{U}_t = [n]$ .

#### 3.1 Optimal Design Algorithm

The key idea is to label examples in  $\mathcal{X}_{\text{examples}}$  that minimize the maximum uncertainty of predictions over all test examples  $\mathbf{x}_{*,k}$ . Our computation of uncertainty is borrowed from linear models. Specifically, take a linear model  $Y = \mathbf{x}^\top \boldsymbol{\theta}_* + \varepsilon$ , where  $\boldsymbol{\theta}_* \in \mathbb{R}^d$  is its parameter and  $\varepsilon \sim \mathcal{N}(0, \sigma^2)$  is independent noise. Suppose that  $\boldsymbol{\theta}_* \sim \mathcal{N}(\boldsymbol{\theta}_0, \boldsymbol{\Sigma}_0)$ . Then a well-known result in Bayesian statistics [Bishop, 2006] is that the posterior variance of the model estimate at an example  $\mathbf{x}_{*,k}$  given labeled examples  $H_t$  is  $\mathbf{x}_{*,k}^\top \widehat{\Sigma}_t \mathbf{x}_{*,k}$ , where  $\widehat{\Sigma}_t = (\boldsymbol{\Sigma}_0^{-1} + \sigma^{-2} \sum_{\ell=1}^{t-1} X_\ell X_\ell^\top)^{-1}$  is the posterior covariance of  $\boldsymbol{\theta}_* \mid H_t$ . Therefore, the maximum uncertainty over test examples is  $\max_{k \in [K]} \mathbf{x}_{*,k}^\top \widehat{\Sigma}_t \mathbf{x}_{*,k}$ . The key observation is that this quantity does not depend on labels. Therefore, it can be optimized greedily by choosing the training example that minimizes it the most,

$$I_t = \arg \min_{i \in \mathcal{U}_t} \max_{k \in [K]} \mathbf{x}_{*,k}^\top \left( \widehat{\Sigma}_t^{-1} + \mathbf{x}_i \mathbf{x}_i^\top \right)^{-1} \mathbf{x}_{*,k}, \quad (1)$$

where  $\mathcal{U}_t$  are indices of all unlabeled training examples up to round  $t$ . After the index  $I_t$  is chosen, the example  $\mathbf{x}_{I_t}$  and its label  $Y_t$  are added to the history to get  $H_{t+1}$  for the next iteration  $t + 1$ .

This algorithm is a greedy solution to the G-optimal design [Pukelsheim, 2006, Katz-Samuels et al., 2021]. We call it **G-Optimal** design and abbreviate it as **GO**. The pseudocode of **GO** is in Algorithm 1. Note that **GO** does not depend on observed  $Y_t$ . Similar optimal designs have been effectively applied in active learning [Chaudhuri et al., 2015, Mukherjee et al., 2022], bandits [Fontaine et al., 2021, Mason et al., 2021], and reinforcement learning [Wagenmaker et al., 2022]. However, this is the first paper that studies optimal design for adaptively designing prompts [Zhang et al., 2022a, Diao et al., 2023]. (1) can be viewed as choosing that training example  $\mathbf{x}_i \in \mathcal{U}_t$  that minimizes the maximum eigenvalue of the posterior covariance  $\widehat{\Sigma}_t$ . Therefore this leads to reducing the uncertainty over the model parameter  $\boldsymbol{\theta}_*$  as the confidence ellipsoid around  $\boldsymbol{\theta}_*$  shrinks [Lattimore and Szepesvári, 2020]. Note that maximum eigenvalue reduction also ensures diversity as it leads to choosing training examples along all directions in  $\mathbb{R}^d$ .

The time complexity of **GO** is  $O(Kd^2nT)$ . This is because, for  $T$  rounds, the algorithm searches for the best training example out of at most  $n$  and evaluates it on all test examples  $\mathbf{x}_{*,k} \in \mathcal{X}_*$ . The evaluation of each test example in round  $t$ ,  $\mathbf{x}_{*,k}^\top (\widehat{\Sigma}_t^{-1} + \mathbf{x}_i \mathbf{x}_i^\top)^{-1} \mathbf{x}_{*,k}$ , takes  $O(d^2)$  time, because  $(\widehat{\Sigma}_t^{-1} + \mathbf{x}_i \mathbf{x}_i^\top)^{-1}$  can be computed in  $O(d^2)$  time using the Sherman-Morrison formula. In the last step, the **LLM** is queried  $K$  times to return  $\{Y_{*,k}\}_{k=1}^K$ .

---

**Algorithm 2** Simulation-based active learning (SAL)
 

---

```

1: Input: Training set  $\mathcal{X}_{\text{examples}} = \{\mathbf{x}_i\}_{i=1}^n$ , test set  $\mathcal{X}_* = \{\mathbf{x}_{*,k}\}_{k=1}^K$ , budget  $T$ 
2:  $\mathcal{L}_1 \leftarrow \emptyset$ ,  $\mathcal{U}_1 \leftarrow [n]$ ,  $H_1 \leftarrow \{\}$ 
3: for  $t = 1, \dots, T$  do
4:   for all  $i \in \mathcal{U}_t$  do
5:     for all  $\mathbf{x}_{*,k} \in \mathcal{X}_*$  do
6:       for  $j = 1, 2, \dots, m$  do
7:         Sample  $Y_{t,i}^{(j)} \sim p(\cdot \mid \mathbf{x}_i, H_t)$ 
8:          $H_{t,i,j} \leftarrow H_t \cup \{(\mathbf{x}_i, Y_{t,i}^{(j)})\}$ 
9:         Sample  $\tilde{Y}_{t,i,k}^{(j,1)}, \tilde{Y}_{t,i,k}^{(j,2)} \sim p(\cdot \mid \mathbf{x}_{*,k}, H_{t,i,j})$ 
10:        end for
11:       end for
12:     end for
13:      $I_t \leftarrow \arg \min_{i \in \mathcal{U}_t} \max_{k \in [K]} \frac{1}{m} \sum_{j=1}^m \left( \tilde{Y}_{t,i,k}^{(j,1)} - \tilde{Y}_{t,i,k}^{(j,2)} \right)^2$ 
14:      $X_t \leftarrow \mathbf{x}_{I_t} \in \mathcal{X}_{\text{examples}}$ 
15:     Observe label  $Y_t$  of example  $X_t$ 
16:      $\mathcal{L}_{t+1} \leftarrow \mathcal{L}_t \cup \{I_t\}$ ,  $\mathcal{U}_{t+1} \leftarrow \mathcal{U}_t \setminus \{I_t\}$ 
17:      $H_{t+1} \leftarrow H_t \cup \{(X_t, Y_t)\}$ 
18:   end for
19: Output: Sample  $Y_{*,k} \sim p(\cdot \mid \mathbf{x}_{*,k}, H_{T+1})$  for  $k \in [K]$ 

```

---

### 3.2 Simulation-Based Algorithm

While **GO** reduces uncertainty in label predictions, it has a major limitation. The chosen example  $X_t$  at round  $t$  is not affected by observed labels  $(Y_\ell)_{\ell \in [t-1]}$ . This is because (1) does not depend on  $(Y_\ell)_{\ell \in [t-1]}$ . While this is a property of linear models, it is undesirable in non-linear models, such as **LLMs**. To address this limitation, we propose a new algorithm that simulates the impact of labeling examples on the uncertainty of predicted labels. We call it **Simulation-Based Active Learning** and abbreviated it as **SAL**. The pseudocode of **SAL** is provided in Algorithm 2.

The key idea in **SAL** is to replace the closed-form formula in (1) by a simulation. We detail the algorithm next. Fix round  $t$ , history  $H_t$ , and candidate example  $\mathbf{x}_i$ . To estimate the impact of labeling  $\mathbf{x}_i$ , we simulate its labels  $m$  times. For each simulation  $j \in [m]$ , we sample  $Y_{t,i}^{(j)}$  from the conditional distribution  $p(\cdot \mid \mathbf{x}_i, H_t)$  using the **LLM**. Then we extend the history  $H_t$  by  $\mathbf{x}_i$  and its simulated label  $Y_{t,i}^{(j)}$ ,  $H_{t,i,j} = H_t \cup \{(\mathbf{x}_i, Y_{t,i}^{(j)})\}$ . This process results in  $m$  copies of augmented histories, each reflecting a potential outcome of labeling of  $\mathbf{x}_i$ . Finally, we take two independent samples for each  $j \in [m]$  as  $\tilde{Y}_{t,i,k}^{(j,1)}, \tilde{Y}_{t,i,k}^{(j,2)} \sim p(\cdot \mid \mathbf{x}_{*,k}, H_{t,i,j})$ . The maximum uncertainty over test examples after labeling  $\mathbf{x}_i$  is estimated as

$$\max_{k \in [K]} \frac{1}{m} \sum_{j=1}^m \left( \tilde{Y}_{t,i,k}^{(j,1)} - \tilde{Y}_{t,i,k}^{(j,2)} \right)^2. \quad (2)$$

The training example with the lowest value is chosen and we denote its index by  $I_t$ . Then  $\mathbf{x}_{I_t}$  and its observed label  $Y_t$  are added to the history to get  $H_{t+1}$  for the next iteration  $t+1$ .

Next we justify **SAL**. Consider the same setting as in Section 3.1. Given a label  $Y_{t,i}^{(j)}$  for example  $\mathbf{x}_i$ , the posterior distribution of  $\theta_* \mid H_{t,i,j}$  is  $\mathcal{N}(\hat{\theta}_{t,i,j}, \hat{\Sigma}_{t,i})$ , where  $\hat{\Sigma}_{t,i} = (\hat{\Sigma}_t^{-1} + \sigma^{-2} \mathbf{x}_i \mathbf{x}_i^\top)^{-1}$  is the simulated posterior covariance of  $\theta_*$  and

$$\hat{\theta}_{t,i,j} = \hat{\Sigma}_{t,i} \left( \hat{\Sigma}_0^{-1} \theta_0 + \sigma^{-2} \left( \sum_{\ell=1}^{t-1} X_\ell Y_\ell + \mathbf{x}_i Y_{t,i}^{(j)} \right) \right)$$

is the posterior mean. By design,  $\tilde{Y}_{t,i,k}^{(j,1)}$  and  $\tilde{Y}_{t,i,k}^{(j,2)}$  are independent samples from  $\mathcal{N}(\mathbf{x}_{*,k}^\top \theta_*, \sigma^2)$ , where  $\theta_* \sim \mathcal{N}(\hat{\theta}_{t,i,j}, \hat{\Sigma}_{t,i})$ . Therefore,  $\tilde{Y}_{t,i,k}^{(j,1)} - \tilde{Y}_{t,i,k}^{(j,2)} \sim \mathcal{N}(0, 2(\mathbf{x}_{*,k}^\top \hat{\Sigma}_{t,i} \mathbf{x}_{*,k} + \sigma^2))$ . By definition,

$(\tilde{Y}_{t,i,k}^{(j,1)} - \tilde{Y}_{t,i,k}^{(j,2)})^2$  is a single sample estimate of  $2(\mathbf{x}_{*,k}^\top \widehat{\Sigma}_{t,i} \mathbf{x}_{*,k} + \sigma^2)$  and the sum in (2) estimates this quantity from  $m$  samples. Note that this estimate is proportional to  $\mathbf{x}_{*,k}^\top \widehat{\Sigma}_{t,i} \mathbf{x}_{*,k}$  that appears in the G-optimal design objective in (1). Therefore, in linear models, SAL can be viewed as an inefficient implementation of GO. This inefficiency stems from the need to simulate the LLM.

The time complexity of SAL is  $O(nKmT)$ . This is because it searches for the best example out of at most  $n$  in  $T$  rounds for each test example  $k \in [K]$ . The evaluation of impact on each test example requires  $2m$  LLM queries.

**Vector labels:** GO and SAL are easy to extend to vector labels,  $d_y > 1$ . GO does not depend on labels at all. The only modification in SAL is that (2) is replaced with  $\max_{k \in [K]} \frac{1}{m} \sum_{j=1}^m \|\tilde{Y}_{t,i,k}^{(j,1)} - \tilde{Y}_{t,i,k}^{(j,2)}\|_2^2$ . This is the sum of the posterior variances of the labels over all dimensions.

## 4 Analysis

In this section, we analyze GO and SAL. The analysis is under the assumption that the labels are scalar and hence, our objective simplifies to minimizing  $\max_{k \in [K]} \text{var}[Y_{*,k} \mid \mathbf{x}_{*,k}, H_{T+1}]$ . The analysis is organized as follows. First, we prove that our objective is decreasing in history but not supermodular, which precludes a straightforward analysis. This property of our objective function is proved in Appendix B.1 and Appendix B.2. Second, we analyze GO using the closed form of the posterior covariance  $\widehat{\Sigma}_t$ . Finally, we prove the equivalence of GO and SAL, and thereby provide guarantees for SAL. All analyses are under the assumption of a linear model with Gaussian noise. These proofs are in Appendix B.3 and Appendix B.4.

### 4.1 Analysis of GO

To address challenge posed due to  $f$  not being a supermodular (Lemma 5), we leverage the properties of the rank-1 updates in GO. The proof is under the assumption that at round  $t$ , the training examples can be partitioned as  $\mathcal{X} = S_k \cup \bar{S}_k$ . The set  $S_k$  represents examples that are close to  $\mathbf{x}_{*,k}$ . The set  $S_k$  is convex such that for a  $\alpha_k \geq 0$  we have  $\mathbf{x}^\top \mathbf{y} \geq \alpha_k$  for all  $\mathbf{x}, \mathbf{y} \in S_k$ . In essence,  $\alpha_k$  governs the minimum level of similarity required for examples within  $S_k$  to be considered similar to the test example  $\mathbf{x}_{*,k}$ . This is achieved by setting a lower bound on the inner product between any two examples in the set. The set  $\bar{S}_k$  represents examples that are not close to  $\mathbf{x}_{*,k}$ . It is defined  $\beta_k \geq 0$  such that  $\mathbf{x}^\top \mathbf{y} \leq \beta_k$  for all  $\mathbf{x} \in S_k$  and  $\mathbf{y} \in \bar{S}_k$ . In contrast to  $\alpha_k$ ,  $\beta_k$  limits the maximum similarity any example in  $S_k$  can have with examples outside this set. Define  $\alpha_{\min} = \min_k \alpha_k$ , and  $\beta_{\max} = \beta_{\max}$ . Define the set  $S = \cap_{k=1}^K S_k$  as the set of all examples that are close to all  $\{\mathbf{x}_{*,k}\}_{k=1}^K$  and  $\bar{S} = \cup_{k=1}^K \bar{S}_k$  as the set of all examples that are not close to all  $\{\mathbf{x}_{*,k}\}_{k=1}^K$ . Assume  $S \neq \{\emptyset\}$  and  $|S| > T$ . With this in hand, we prove the following claim.

**Theorem 1.** *Let  $\alpha_{\min}, \beta_{\max} \geq 0$  be set such that  $\beta_{\max} \geq 1 - \alpha_{\min}^2$  and  $T \leq \frac{\alpha_{\min}^2}{(\beta_{\max} + \sqrt{2})\beta_{\max}d}$ . Then for any  $\mathbf{x}_{*,k}$  we can show that  $\mathbf{x}_{*,k}^\top \widehat{\Sigma}_{T+1} \mathbf{x}_{*,k} \leq \frac{1}{\alpha_{\max}^2 T+1} + (1 - \alpha_{\max}^2)$ .*

The proof is in Appendix B.3. It is a major departure from similar proofs in active learning with a fixed budget [Tong and Koller, 2001, Hanneke et al., 2014, Azizi et al., 2022, Yang and Tan, 2022] in three aspects. First, we analyze the discrete allocation problem in (3) instead of its continuous optimal-design relaxation [Pukelsheim, 2006]. Second, any unlabeled example in  $\mathcal{X}$  is labeled at most once. Finally, (3) is asymmetric in the sense that we optimize the uncertainty of a single example  $\mathbf{x}_*$  over a larger set. To make the analysis manageable, we impose structure on  $\mathcal{X}$ . The claim in Theorem 1 holds for any  $T$  if  $\beta_{\max} = 1/(4dn)$  and  $\alpha_{\min} = \sqrt{1 - \beta_{\max}}$ . In this case,  $\alpha_{\min}$  is close to 1, and we get a near-optimal  $O(1/T)$  decrease in posterior variance.

### 4.2 Analysis of SAL

For a sufficiently large sample size  $m$  in SAL, we can establish the following equivalence of SAL and GO.

**Theorem 2.** *Fix a failure probability  $\delta \in (0, 1)$ . Define  $\sigma_{t,i,k}^2 = \mathbb{E}[\frac{1}{m} \sum_{j=1}^m (\tilde{Y}_{t,i,k}^{(j,1)} - \tilde{Y}_{t,i,k}^{(j,2)})^2] = 2\mathbf{x}_{*,k}^\top \widehat{\Sigma}_{t,i} \mathbf{x}_{*,k} + \sigma^2$ , and define  $\sigma_{t,i,\max}^2 = \max_{k \in [K]} \sigma_{t,i,k}^2$ . Then for any  $t \in [T]$  and  $i \in \mathcal{U}_t$ , we*

have that

$$\sigma_{t,i,\max}^2 \left[ 1 - 2\sqrt{\frac{\log(1/\delta)}{m}} \right] \leq \max_{k \in [K]} \frac{1}{m} \sum_{j=1}^m \left( \tilde{Y}_{t,i,k}^{(j,1)} - \tilde{Y}_{t,i,k}^{(j,2)} \right)^2 \leq \sigma_{t,i,\max}^2 \left[ 1 + 2\sqrt{\frac{\log(1/\delta)}{m}} + \frac{2\log(1/\delta)}{m} \right].$$

Moreover, for  $m \geq 8 \log(1/\delta)$  we have that

$$2 \max_k \mathbf{x}_{*,k}^\top \widehat{\Sigma}_{t,i} \mathbf{x}_{*,k} + \frac{\sigma^2}{2} \leq \max_k \frac{1}{m} \sum_{j=1}^m \left( \tilde{Y}_{t,i,k}^{(j,1)} - \tilde{Y}_{t,i,k}^{(j,2)} \right)^2 \leq 5 \max_k \mathbf{x}_{*,k}^\top \widehat{\Sigma}_{t,i} \mathbf{x}_{*,k} + \frac{5\sigma^2}{2}.$$

These claims hold with probability at least  $1 - \delta$ .

The claim is proved in Appendix B.4. The key idea in the proof is that (2) multiplied by  $m/[2(\mathbf{x}_{*,k}^\top \widehat{\Sigma}_{t,i} \mathbf{x}_{*,k} + \sigma^2)]$  is a chi-squared random variable with  $m$  degrees of freedom. Then we use concentration inequalities of Laurent and Massart [2000] to get a high-probability confidence interval on distance to the mean  $m$ , which in turn allows us to relate the actual variance to its empirical estimate. Theorem 2 shows that SAL is equivalent to GO for a sufficiently large sample size  $m$ . Theorem 1 can be then adapted to SAL as follows. The only change is in condition on  $T$ , which changes to  $T \leq \alpha^2 / \left( \beta + \sqrt{2} O \left( \frac{1 - \sqrt{1/m}}{1 + \sqrt{1/m}} \right) \right) \beta d + O(\sqrt{1/m})$ . Therefore, SAL attains a near-optimal  $O(1/T)$  decrease in posterior variance as  $m \rightarrow \infty$ .

## 5 Experiments

We evaluate GO and SAL on a variety of prediction tasks. These tasks cover both classification and regression, including natural language features, and help us to evaluate the capabilities of GO and SAL to choose few-shot examples for active in-context prompt design. We also demonstrate that GO and SAL can be used for general pattern recognition. Detailed descriptions of all datasets are in Appendix C.1. We describe the prompts in detail in Appendix D.

### 5.1 Experimental Setup

We use Mistral-7B [Jiang et al., 2023], Vicuna-13B [Chiang et al., 2023], and Falcon-40B [Penedo et al., 2023] as the LLMs and design prompts following Dinh et al. [2022] and Suzgun et al. [2022]. To investigate the impact of LLM model size on performance, we experiment with these three models of varying sizes: 7B, 13B, and 40B. Interestingly, we observe that the smaller models (Mistral-7B and Vicuna-13B) perform very poorly on certain tasks. Examples of the prompts are given in Appendix D. Each experiment is averaged over 10 trials. At the beginning of each trial, we randomly select  $K = 20$  test examples. We describe in detail how the training set and  $n$  are chosen for each dataset in Appendix C.

Each run is a simulation that proceeds as follows. In round  $t$ , each method selects a training example to label  $X_t$  and then observes the true label  $Y_t$ . All past interactions  $H_t = \{(X_\ell, Y_\ell)\}_{\ell \in [t-1]}$  along with the test examples  $\mathbf{x}_{*,k}$  are used to craft a prompt for the LLM. The performance at round  $t$  is evaluated by the error  $\mathcal{L}(t) = \frac{1}{K} \sum_{k=1}^K \mathcal{L}(Y_{*,k}, \tilde{Y}_{*,k,t})$ , where  $Y_{*,k}$  is the true label of test example  $\mathbf{x}_{*,k}$ ,  $\tilde{Y}_{*,k,t}$  is its LLM predicted label in round  $t$ , and  $\mathcal{L}(y_*, y)$  is a task-specific error function. For classification tasks, we choose  $\mathcal{L}(y_*, y) = \mathbb{I}\{y_* = y\}$  and call  $\mathcal{L}(t)$  a *misclassification error*. For regression tasks, we choose  $\mathcal{L}(y_*, y) = (y_* - y)^2$  and call  $\mathcal{L}(t)$  the *MSE*. For pattern recognition tasks, where  $Y_{*,k}$  and  $\tilde{Y}_{*,k,t}$  are either vectors or matrices, we choose let  $\mathcal{L}(y_*, y) = \mathbb{I}\{y_* = y\}$  and  $\mathcal{L}(t)$  represents *0-1 error*.

We posit that GO and SAL perform well because they both reduce the uncertainty of test examples based on the right notion of similarity. To show this, we compare to baselines that reduce uncertainty uniformly (like Uniform), or reduce uncertainty informatively (Least or Max-Entropy), or only select examples with similar features to test examples (Greedy-NN). As shown in our extensive experiments, these baselines fail to match the capabilities of GO and SAL to select informative examples in the majority of the tasks. The following methods are compared in our experiments:

**(1) Uniform:** The example  $X_t$  in round  $t$  is sampled uniformly at random from the unlabeled set  $\mathcal{U}_t$ . Uniform is a pure exploration algorithm that does not take into account the similarity to test examples and variance reduction. We chose it as a baseline because it tends to work well in practice. Therefore,

	Datasets	Uniform	Greedy-NN	Least	Max-Entropy	GO (ours)	SAL (ours)
M	iris	0.41 ± 0.11	0.60 ± 0.13	0.64 ± 0.15	0.72 ± 0.17	0.38 ± 0.14	<b>0.34 ± 0.14</b>
	banknote	0.75 ± 0.10	<b>0.58 ± 0.04</b>	0.59 ± 0.02	0.73 ± 0.16	0.77 ± 0.07	0.75 ± 0.15
	balance-scale	0.61 ± 0.13	0.69 ± 0.22	0.55 ± 0.25	0.57 ± 0.14	<b>0.48 ± 0.09</b>	0.72 ± 0.04
	thyroid-new	<b>0.44 ± 0.12</b>	0.70 ± 0.08	0.74 ± 0.12	0.57 ± 0.08	0.55 ± 0.06	0.63 ± 0.14
V	iris	0.22 ± 0.24	0.60 ± 0.37	0.60 ± 0.49	0.40 ± 0.20	0.20 ± 0.24	<b>0.20 ± 0.24</b>
	banknote	0.40 ± 0.37	0.80 ± 0.24	0.50 ± 0.32	0.50 ± 0.32	0.50 ± 0.32	<b>0.10 ± 0.20</b>
	balance-scale	0.60 ± 0.20	0.60 ± 0.37	0.50 ± 0.32	0.80 ± 0.24	<b>0.30 ± 0.24</b>	0.50 ± 0.00
	thyroid-new	0.52 ± 0.45	1.00 ± 0.00	0.70 ± 0.24	0.50 ± 0.00	0.60 ± 0.20	<b>0.50 ± 0.32</b>
F	iris	<b>0.20 ± 0.06</b>	0.62 ± 0.14	0.70 ± 0.20	0.65 ± 0.18	0.42 ± 0.10	0.33 ± 0.23
	banknote	0.45 ± 0.23	0.53 ± 0.25	0.60 ± 0.12	0.42 ± 0.17	0.45 ± 0.06	<b>0.45 ± 0.1</b>
	balance-scale	0.70 ± 0.28	0.68 ± 0.13	0.85 ± 0.12	0.62 ± 0.08	0.47 ± 0.24	<b>0.45 ± 0.13</b>
	thyroid-new	0.55 ± 0.29	0.57 ± 0.20	0.75 ± 0.19	0.65 ± 0.15	0.55 ± 0.23	<b>0.53 ± 0.12</b>

Table 1: Misclassification error in classification datasets using Mistral-7B (M), Vicuna-13B (V), and Falcon-40B (F) on  $K = 20$  test examples at the end of budget  $T = 5$ .

	Datasets	Uniform	Greedy-NN	Least	Max-Entropy	GO (ours)	SAL (ours)
M	machine(e+04)	11.4 ± 3.34	10.5 ± 2.44	14.3 ± 3.39	11.0 ± 1.93	<b>10.5 ± 3.74</b>	10.6 ± 3.84
	fifa(e-04)	1.40 ± .216	3.72 ± 1.12	1.18 ± .53	4.15 ± 1.11	.999 ± .404	<b>.68 ± .26</b>
V	machine(e+04)	5.59 ± 1.35	5.04 ± .851	7.95 ± 1.69	4.98 ± 1.06	5.66 ± 1.54	<b>4.80 ± 1.46</b>
	fifa(e+03)	5.90 ± 1.59	4.72 ± .931	5.11 ± 1.12	6.76 ± 1.69	<b>1.44 ± .258</b>	2.59 ± .742
F	machine(e+03)	1.16 ± 1.22	4.28 ± 2.30	2.15 ± 1.08	3.50 ± 2.45e + 03	.32 ± .209	<b>2.96 ± 1.56</b>
	fifa(e+01)	7.78 ± 3.85	6.95 ± 2.93	12.4 ± 12.3	26.3 ± 37.6	7.90 ± 4.64	<b>4.61 ± 4.35</b>

Table 2: MSE in regression datasets using Mistral-7B (M), Vicuna-13B (V), and Falcon-40B (F) on  $K = 20$  test examples at the end of budget  $T = 5$ .

it is used frequently in active learning and prompt tuning papers [Zhang et al., 2022b, Diao et al., 2023].

(2) **Greedy-NN**: The example  $X_t$  in round  $t$  is chosen to align the most with all test examples  $\mathbf{x}_{*,k}$  such that  $I_t \leftarrow \arg \max_{i \in \mathcal{U}_t} \max_{k \in [K]} \mathbf{x}_{*,k}^\top \mathbf{x}_i$ . This baseline shows that our information gathering rule in (1) goes beyond pure feature similarity. This baseline is similar to the automatic exemplar construction method by clustering by Zhang et al. [2022b].

(3) **Least**: This is similar to the disagreement-based method of Diao et al. [2023]. The disagreement score of the example  $i \in \mathcal{U}_t$  is calculated as  $s_i = \sum_{k=1}^K Y_{tik}$  where  $Y_{tik} \sim p(\cdot | \mathbf{x}_{*,k}, \mathbf{x}_i)$  is the number of unique answers by for test example  $\mathbf{x}_{*,k}$  using only  $\mathbf{x}_i$  as the in-context example by the LLM. Then the example selected at round  $t$  is  $I_t \leftarrow \arg \max_{i \in \mathcal{U}_t} s_i$ . This is the unlabeled example where the LLM, disagrees the most for all test examples and is least confident. We compare against this baseline to show that our information gathering rule in (1) goes beyond just uncertainty sampling but also takes into account the diversity of training examples when choosing to label the next example.

(4) **Max-Entropy**: This is the uncertainty-based maximum entropy method of Zhang et al. [2022a], Diao et al. [2023]. At round  $t$  the example with the highest entropy is selected as  $I_t \leftarrow \arg \max_{i \in \mathcal{U}_t} - \sum_{k=1}^K \bar{Y}_{tik} \ln \bar{Y}_{tik}$  where  $\bar{Y}_{tik} \sim p(\cdot | \mathbf{x}_{*,k}, \mathbf{x}_i)$  is the frequency of a predicted answer among all predictions for the test example  $\mathbf{x}_{*,k}$  using  $\mathbf{x}_i$  as the in-context example by the LLM. A larger entropy denotes greater uncertainty and therefore, an unlabeled example with the largest entropy will be selected. Again we compare against this uncertainty-based baseline to show that our information gathering rule in (1) goes beyond just uncertainty sampling but also considers the diversity of training examples when choosing to label the next example.

(5) **GO (ours)**: This is Algorithm 1 where  $\mathcal{X}$  are the original feature vectors.

(6) **GO-Inst (ours)**: This is Algorithm 1 where the original feature vectors are used in the prompt but  $\mathcal{X}$  are their 768-dimensional Instructor embeddings [Su et al., 2022]. We use this for natural language classification tasks.

(7) **SAL (ours)**: This is Algorithm 2 where  $\mathcal{X}$  are the original feature vectors. To implement SAL efficiently, we combine it with GO as a preprocessing step. Specifically, in round  $t$ , GO first chooses 5 most informative examples from  $\mathcal{U}_t$  and then we apply SAL. We use  $m = 1$  in all experiments. We use these approximations because SAL is computationally expensive (Section 3.2). Similarly to GO-Inst, we use Instructor embeddings for natural language classification tasks.

All used datasets and experimental setups are described in Appendix C. This section only summarizes the main results.

Task	Uniform	Greedy-NN	Least	Max-Entropy	GO (ours)	SAL (ours)
Arc-1	0.45 ± 0.50	0.45 ± 0.50	0.90 ± 0.30	0.60 ± 0.49	0.30 ± 0.46	<b>0.15 ± 0.36</b>
Arc-2	0.80 ± 0.40	1.00 ± 0.00	0.80 ± 0.40	0.80 ± 0.40	0.80 ± 0.40	<b>0.01 ± 0.01</b>
PCFG-1	0.60 ± 0.49	1.00 ± 0.00	1.00 ± 0.00	1.00 ± 0.01	0.20 ± 0.40	<b>0.02 ± 0.01</b>
PCFG-2	0.20 ± 0.40	1.00 ± 0.00	0.20 ± 0.40	1.00 ± 0.00	0.20 ± 0.40	<b>0.14 ± 0.40</b>

Table 3: 0-1 error using Falcon-40B on  $K = 20$  test examples at the end of budget  $T = 5$ . ARC-1 is the expansion-contraction task, ARC-2 is the rotation task, PCFG-1 is the add-subtract task, and PCFG-2 is the repeat experiment task. Mistral-7B and Vicuna-13B perform very poorly on these tasks and thus are omitted.

Datasets		Uniform	Greedy-NN	Least	Max-Entropy	GO (ours)	SAL (ours)
M	movie	0.32 ± 0.17	0.90 ± 0.06	0.87 ± 0.09	0.55 ± 0.18	<b>0.27 ± 0.10</b>	0.49 ± 0.11
	entity	0.69 ± 0.19	0.86 ± 0.06	0.87 ± 0.09	0.59 ± 0.15	0.65 ± 0.18	<b>0.39 ± 0.19</b>
	theme	0.74 ± 0.05	0.74 ± 0.09	0.82 ± 0.16	<b>0.68 ± 0.09</b>	0.80 ± 0.09	0.81 ± 0.08
V	movie	0.10 ± 0.20	0.70 ± 0.24	0.90 ± 0.20	0.30 ± 0.24	<b>0.02 ± 0.01</b>	0.10 ± 0.20
	entity	0.20 ± 0.24	0.90 ± 0.20	0.70 ± 0.24	0.60 ± 0.20	<b>0.10 ± 0.20</b>	0.10 ± 0.20
	theme	0.90 ± 0.20	0.70 ± 0.40	1.00 ± 0.00	0.70 ± 0.24	<b>0.60 ± 0.37</b>	0.80 ± 0.40
F	movie	0.55 ± 0.06	0.62 ± 0.18	0.78 ± 0.17	0.53 ± 0.22	<b>0.38 ± 0.18</b>	0.47 ± 0.17
	entity	0.55 ± 0.23	0.62 ± 0.08	0.75 ± 0.14	0.65 ± 0.24	0.47 ± 0.23	<b>0.42 ± 0.24</b>
	theme	0.68 ± 0.20	0.70 ± 0.13	0.85 ± 0.05	0.85 ± 0.09	<b>0.53 ± 0.18</b>	0.55 ± 0.19

Table 4: Misclassification error in natural language classification tasks using Mistral-7B (M), Vicuna-13B (V), and Falcon-40B (F) on  $K = 20$  test examples at the end of budget  $T = 5$ .

**Standard classification and regression tasks.** We use 4 classification and 2 regression datasets from UCI and OpenML (Appendix C.1). We set  $T = 5$  to simulate the realistic scenario when the test queries provided by the user need to be inferred quickly. For classification tasks,  $K = 20$  test examples are chosen among the different classes of the dataset. We describe in detail how the training set and  $n$  are chosen for each dataset in Appendix C. For regression tasks,  $K = 20$  random test examples are chosen. Our results on classification tasks are reported in Table 1 and on regression tasks in Table 2. We observe that GO and SAL are the best-performing methods in the majority of the datasets. Note that there is no single baseline that consistently outperforms them.

**General pattern recognition.** We experiment with 4 tasks: ARC expansion and contraction, ARC rotation, PCFG Add-Subtract, and PCFG Repeat. Both inputs and outputs in these tasks are vectors or matrices. We describe examples of ARC and PCFG tasks in detail in Appendix C.1. Each dataset comprises examples of two patterns: expansion and contraction, clockwise and counter-clockwise rotation, add and subtract, repeat first and second digits. In each trial, we choose  $K = 20$  different test examples equally from two patterns and set  $T = 5$ . Our results are reported in Table 3. In all tasks, GO and SAL are the best-performing methods. SAL outperforms GO in ARC [Alford, 2021, Mirchandani et al., 2023] and PCFG [Hupkes et al., 2020] consistently.

**Natural language classification tasks (NLC).** We show that GO and SAL work well on general NLP tasks where no explicit numerical features are available. We create three synthetic datasets based on the following tasks: (i) `movie-names`: predicting a genre from a movie name (e.g., romance, horror), (ii) `movie-theme`: predicting a common theme for a pair of movie names (e.g., coming-of-age, sci-fi), and (iii) `entity-names`: predicting an entity’s type from its name (e.g., celebrity, mountain, river). Each dataset comprises 5 classes. Further details regarding the additional datasets are provided in Appendix C. In each trial,  $K = 20$  test examples were randomly chosen across the five classes. The feature vectors in GO and SAL are Instructor embeddings of the original text features. Our results are reported in Table 4. We observe again that GO and SAL are the best-performing methods in the majority of the datasets. There is no single baseline that consistently outperforms them. This shows that the optimal design-based approach of GO and SAL correctly balances uncertainty and diversity-based sampling.

## 6 Conclusions

In this paper, we studied the framework of active in-context prompt design (AIPD) that uses optimal design to systematically choose the most informative unlabeled examples to label for a set of test examples. These informative labeled examples are then used to minimize the prediction error of the LLM for all the test examples. To our knowledge, this is the first paper that studies optimal design for adaptive prompt design. Inspired by the linear model, we proposed an algorithm GO that strategically chooses the most informative examples that minimize the variance of the posterior covariance for any test example from the test set. We proposed a second algorithm SAL that uses simulations to estimate the impact of how unlabeled examples reduce LLM uncertainty for all test examples. It then chooses to label examples that maximally reduce the uncertainty of the LLM for all

test examples from the test set. We theoretically analyze **GO** and **SAL** and show their equivalence in linear models. We show that both algorithms guarantee information gain at each iteration. Finally, we show empirically that, when used with **LLMs** like Mistral-7B, Vicuna-13B, and Falcon-40B, both **GO** and **SAL** result in better prediction accuracy than other baselines [Zhang et al., 2022a,b, Diao et al., 2023] on tasks like classification, regression, ARC, PCFG, and natural language generation. Our research opens up exciting new directions for future work such as extending **AIPD** framework beyond text to enable informative example selection for tasks involving images, videos, or other modalities using multi-modal **LLMs** [Yin et al., 2023]. Additionally, the integration of active learning with diffusion models, a powerful class of generative models, presents promising directions for future research [Ho et al., 2020].

## References

- Simon Alford. *A Neurosymbolic Approach to Abstraction and Reasoning*. PhD thesis, Massachusetts Institute of Technology, 2021.
- David Arthur and Sergei Vassilvitskii. k-means++: The advantages of careful seeding. Technical report, Stanford, 2006.
- Jordan Ash, Surbhi Goel, Akshay Krishnamurthy, and Sham Kakade. Gone fishing: Neural active learning with fisher embeddings. *Advances in Neural Information Processing Systems*, 34, 2021.
- Jordan T Ash, Chicheng Zhang, Akshay Krishnamurthy, John Langford, and Alekh Agarwal. Deep batch active learning by diverse, uncertain gradient lower bounds. *arXiv preprint arXiv:1906.03671*, 2019.
- Mohammad Javad Azizi, Branislav Kveton, and Mohammad Ghavamzadeh. Fixed-budget best-arm identification in structured bandits. In *Proceedings of the 31st International Joint Conference on Artificial Intelligence*, 2022.
- Yu Bai, Fan Chen, Huan Wang, Caiming Xiong, and Song Mei. Transformers as statisticians: Provable in-context learning with in-context algorithm selection. *arXiv preprint arXiv:2306.04637*, 2023.
- Maria-Florina Balcan, Alina Beygelzimer, and John Langford. Agnostic active learning. *Journal of Computer and System Sciences*, 75(1):78–89, 2009.
- Gantavya Bhatt, Yifang Chen, Arnav M Das, Jifan Zhang, Sang T Truong, Stephen Mussmann, Yinglun Zhu, Jeffrey Bilmes, Simon S Du, Kevin Jamieson, et al. An experimental design framework for label-efficient supervised finetuning of large language models. *arXiv preprint arXiv:2401.06692*, 2024.
- Christopher Bishop. *Pattern Recognition and Machine Learning*. Springer, New York, NY, 2006.
- Benjamin Bowman, Alessandro Achille, Luca Zancato, Matthew Trager, Pramuditha Perera, Giovanni Paolini, and Stefano Soatto. a-la-carte prompt tuning (apt): Combining distinct data via composable prompting. In *Proceedings of the IEEE/CVF Conference on Computer Vision and Pattern Recognition*, pages 14984–14993, 2023.
- Tom Brown, Benjamin Mann, Nick Ryder, Melanie Subbiah, Jared D Kaplan, Prafulla Dhariwal, Arvind Neelakantan, Pranav Shyam, Girish Sastry, Amanda Askell, et al. Language models are few-shot learners. *Advances in neural information processing systems*, 33:1877–1901, 2020a.
- Tom Brown et al. Language models are few-shot learners. In *Advances in Neural Information Processing Systems 33*, 2020b.
- BuoyHealth. BuoyHealth. <https://www.buoyhealth.com/>.
- Loredana Caruccio, Stefano Cirillo, Giuseppe Polese, Giandomenico Solimando, Shanmugam Sundaramurthy, and Genoveffa Tortora. Can chatgpt provide intelligent diagnoses? a comparative study between predictive models and chatgpt to define a new medical diagnostic bot. *Expert Systems with Applications*, 235:121186, 2024. ISSN 0957-4174. doi: <https://doi.org/10.1016/j.eswa.2023.121186>. URL <https://www.sciencedirect.com/science/article/pii/S0957417423016883>.

- Kamalika Chaudhuri, Sham M Kakade, Praneeth Netrapalli, and Sujay Sanghavi. Convergence rates of active learning for maximum likelihood estimation. In *Advances in Neural Information Processing Systems*, pages 1090–1098, 2015.
- Yifang Chen, Yingbing Huang, Simon S Du, Kevin Jamieson, and Guanya Shi. Active representation learning for general task space with applications in robotics. *arXiv preprint arXiv:2306.08942*, 2023.
- Wei-Lin Chiang, Zhuohan Li, Zi Lin, Ying Sheng, Zhanghao Wu, Hao Zhang, Lianmin Zheng, Siyuan Zhuang, Yonghao Zhuang, Joseph E. Gonzalez, Ion Stoica, and Eric P. Xing. Vicuna: An open-source chatbot impressing gpt-4 with 90%\* chatgpt quality, March 2023. URL <https://lmsys.org/blog/2023-03-30-vicuna/>.
- Gui Citovsky, Giulia DeSalvo, Claudio Gentile, Lazaros Karydas, Anand Rajagopalan, Afshin Rostamizadeh, and Sanjiv Kumar. Batch active learning at scale. *Advances in Neural Information Processing Systems*, 34, 2021.
- Sanjoy Dasgupta. Analysis of a greedy active learning strategy. In *Advances in Neural Information Processing Systems 17*, pages 337–344, 2005.
- Sanjoy Dasgupta, Daniel J Hsu, and Claire Monteleoni. A general agnostic active learning algorithm. *Advances in neural information processing systems*, 20, 2007.
- Zhijie Deng, Hongcheng Gao, Yibo Miao, and Hao Zhang. Efficient detection of llm-generated texts with a bayesian surrogate model. *arXiv preprint arXiv:2305.16617*, 2023.
- Jacob Devlin, Ming-Wei Chang, Kenton Lee, and Kristina Toutanova. Bert: Pre-training of deep bidirectional transformers for language understanding. *arXiv preprint arXiv:1810.04805*, 2018.
- Shizhe Diao, Pengcheng Wang, Yong Lin, and Tong Zhang. Active prompting with chain-of-thought for large language models. *arXiv preprint arXiv:2302.12246*, 2023.
- Ning Ding, Yujia Qin, Guang Yang, Fuchao Wei, Zonghan Yang, Yusheng Su, Shengding Hu, Yulin Chen, Chi-Min Chan, Weize Chen, et al. Parameter-efficient fine-tuning of large-scale pre-trained language models. *Nature Machine Intelligence*, 5(3):220–235, 2023.
- Tuan Dinh, Yuchen Zeng, Ruisu Zhang, Ziqian Lin, Michael Gira, Shashank Rajput, Jy-yong Sohn, Dimitris Papailiopoulos, and Kangwook Lee. Lift: Language-interfaced fine-tuning for non-language machine learning tasks. *Advances in Neural Information Processing Systems*, 35: 11763–11784, 2022.
- Qingxiu Dong, Lei Li, Damai Dai, Ce Zheng, Zhiyong Wu, Baobao Chang, Xu Sun, Jingjing Xu, and Zhifang Sui. A survey for in-context learning. *arXiv preprint arXiv:2301.00234*, 2022.
- Yonatan Dukler, Alessandro Achille, Giovanni Paolini, Avinash Ravichandran, Marzia Polito, and Stefano Soatto. Diva: Dataset derivative of a learning task. *arXiv preprint arXiv:2111.09785*, 2021.
- Valerii Vadimovich Fedorov. *Theory of optimal experiments*. Elsevier, 2013.
- Chris Fifty, Ehsan Amid, Zhe Zhao, Tianhe Yu, Rohan Anil, and Chelsea Finn. Efficiently identifying task groupings for multi-task learning. *Advances in Neural Information Processing Systems*, 34: 27503–27516, 2021.
- Xavier Fontaine, Pierre Perrault, Michal Valko, and Vianney Perchet. Online a-optimal design and active linear regression. In *International Conference on Machine Learning*, pages 3374–3383. PMLR, 2021.
- Yarin Gal, Riashat Islam, and Zoubin Ghahramani. Deep Bayesian active learning with image data. In Doina Precup and Yee Whye Teh, editors, *Proceedings of the 34th International Conference on Machine Learning*, volume 70 of *Proceedings of Machine Learning Research*, pages 1183–1192. PMLR, 06–11 Aug 2017. URL <https://proceedings.mlr.press/v70/gal17a.html>.
- Tianshi Gao and Daphne Koller. Active classification based on value of classifier. *Advances in neural information processing systems*, 24, 2011.

- Yonatan Geifman and Ran El-Yaniv. Deep active learning over the long tail. *arXiv preprint arXiv:1711.00941*, 2017.
- Steve Hanneke et al. Theory of disagreement-based active learning. *Foundations and Trends® in Machine Learning*, 7(2-3):131–309, 2014.
- Jameel Hassan, Hanan Gani, Noor Hussein, Muhammad Uzair Khattak, Muzammal Naseer, Fahad Shahbaz Khan, and Salman Khan. Align your prompts: Test-time prompting with distribution alignment for zero-shot generalization. *arXiv preprint arXiv:2311.01459*, 2023.
- Jonathan Ho, Ajay Jain, and Pieter Abbeel. Denoising diffusion probabilistic models. *Advances in neural information processing systems*, 33:6840–6851, 2020.
- Dieuwke Hupkes, Verna Dankers, Mathijs Mul, and Elia Bruni. Compositionality decomposed: How do neural networks generalise? *Journal of Artificial Intelligence Research*, 67:757–795, 2020.
- Albert Q Jiang, Alexandre Sablayrolles, Arthur Mensch, Chris Bamford, Devendra Singh Chaplot, Diego de las Casas, Florian Bressand, Gianna Lengyel, Guillaume Lample, Lucile Saulnier, et al. Mistral 7b. *arXiv preprint arXiv:2310.06825*, 2023.
- Julian Katz-Samuels, Jifan Zhang, Lalit Jain, and Kevin Jamieson. Improved algorithms for agnostic pool-based active classification. In *International Conference on Machine Learning*, pages 5334–5344. PMLR, 2021.
- Jack Kiefer and Jacob Wolfowitz. The equivalence of two extremum problems. *Canadian Journal of Mathematics*, 12:363–366, 1960.
- Andreas Kirsch, Joost Van Amersfoort, and Yarin Gal. Batchbald: Efficient and diverse batch acquisition for deep bayesian active learning. *Advances in neural information processing systems*, 32, 2019.
- Jan Kremer, Kim Steenstrup Pedersen, and Christian Igel. Active learning with support vector machines. *Wiley Interdisciplinary Reviews: Data Mining and Knowledge Discovery*, 4(4):313–326, 2014.
- Po-Nien Kung, Fan Yin, Di Wu, Kai-Wei Chang, and Nanyun Peng. Active instruction tuning: Improving cross-task generalization by training on prompt sensitive tasks. *arXiv preprint arXiv:2311.00288*, 2023.
- Tomoyuki Kuroiwa, Aida Sarcon, Takuya Ibara, Eriku Yamada, Akiko Yamamoto, Kazuya Tsukamoto, and Koji Fujita. The potential of chatgpt as a self-diagnostic tool in common orthopedic diseases: Exploratory study. *J Med Internet Res*, 25:e47621, Sep 2023. ISSN 1438-8871. doi: 10.2196/47621. URL <https://www.jmir.org/2023/1/e47621>.
- Anusha Lalitha Lalitha, Kousha Kalantari, Yifei Ma, Anoop Deoras, and Branislav Kveton. Fixed-budget best-arm identification with heterogeneous reward variances. In *Uncertainty in Artificial Intelligence*, pages 1164–1173. PMLR, 2023.
- Tor Lattimore and Csaba Szepesvári. *Bandit algorithms*. Cambridge University Press, 2020.
- Beatrice Laurent and Pascal Massart. Adaptive estimation of a quadratic functional by model selection. *Annals of statistics*, pages 1302–1338, 2000.
- Jonathan N Lee, Annie Xie, Aldo Pacchiano, Yash Chandak, Chelsea Finn, Ofir Nachum, and Emma Brunskill. Supervised pretraining can learn in-context reinforcement learning. *arXiv preprint arXiv:2306.14892*, 2023.
- Brian Lester, Rami Al-Rfou, and Noah Constant. The power of scale for parameter-efficient prompt tuning. *arXiv preprint arXiv:2104.08691*, 2021.
- David D Lewis. A sequential algorithm for training text classifiers: Corrigendum and additional data. In *Acm Sigir Forum*, volume 29, pages 13–19. ACM New York, NY, USA, 1995.

- Pengfei Liu, Weizhe Yuan, Jinlan Fu, Zhengbao Jiang, Hiroaki Hayashi, and Graham Neubig. Pre-train, prompt, and predict: A systematic survey of prompting methods in natural language processing. *ACM Computing Surveys*, 55(9):1–35, 2023a.
- Yajing Liu, Yuning Lu, Hao Liu, Yaozu An, Zhuoran Xu, Zhuokun Yao, Baofeng Zhang, Zhiwei Xiong, and Chenguang Gui. Hierarchical prompt learning for multi-task learning. In *Proceedings of the IEEE/CVF Conference on Computer Vision and Pattern Recognition*, pages 10888–10898, 2023b.
- livehealthily. livehealthily. <https://www.livehealthily.com/>.
- Katerina Margatina, Timo Schick, Nikolaos Aletras, and Jane Dwivedi-Yu. Active learning principles for in-context learning with large language models. *arXiv preprint arXiv:2305.14264*, 2023.
- Kolby Nottingham Markelle Kelly, Rachel Longjohn. The uci machine learning repository, 1988. URL <https://archive.ics.uci.edu>.
- Blake Mason, Romain Camilleri, Subhojyoti Mukherjee, Kevin Jamieson, Robert Nowak, and Lalit Jain. Nearly optimal algorithms for level set estimation. *arXiv preprint arXiv:2111.01768*, 2021.
- Sewon Min, Xinxu Lyu, Ari Holtzman, Mikel Artetxe, Mike Lewis, Hannaneh Hajishirzi, and Luke Zettlemoyer. Rethinking the role of demonstrations: What makes in-context learning work? *arXiv preprint arXiv:2202.12837*, 2022.
- Suvir Mirchandani, Fei Xia, Pete Florence, Brian Ichter, Danny Driess, Montserrat Gonzalez Arenas, Kanishka Rao, Dorsa Sadigh, and Andy Zeng. Large language models as general pattern machines. *arXiv preprint arXiv:2307.04721*, 2023.
- Subhojyoti Mukherjee, Ardhendu S Tripathy, and Robert Nowak. Chernoff sampling for active testing and extension to active regression. In *International Conference on Artificial Intelligence and Statistics*, pages 7384–7432. PMLR, 2022.
- G. L. Nemhauser, L. A. Wolsey, and M. L. Fisher. An analysis of approximations for maximizing submodular set functions - I. *Mathematical Programming*, 14(1):265–294, 1978.
- Guilherme Penedo, Quentin Malartic, Daniel Hesslow, Ruxandra Cojocaru, Alessandro Cappelli, Hamza Alobeidli, Baptiste Pannier, Ebtesam Almazrouei, and Julien Launay. The RefinedWeb dataset for Falcon LLM: outperforming curated corpora with web data, and web data only. *arXiv preprint arXiv:2306.01116*, 2023. URL <https://arxiv.org/abs/2306.01116>.
- Pramuditha Perera, Matthew Trager, Luca Zancato, Alessandro Achille, and Stefano Soatto. Prompt algebra for task composition. *arXiv preprint arXiv:2306.00310*, 2023.
- Yotam Perlitz, Ariel Gera, Michal Shmueli-Scheuer, Dafna Sheinwald, Noam Slonim, and Liat Ein-Dor. Active learning for natural language generation. *arXiv preprint arXiv:2305.15040*, 2023.
- Friedrich Pukelsheim. *Optimal design of experiments*. SIAM, 2006.
- Pengzhen Ren, Yun Xiao, Xiaojun Chang, Po-Yao Huang, Zhihui Li, Brij B Gupta, Xiaojiang Chen, and Xin Wang. A survey of deep active learning. *ACM Computing Surveys (CSUR)*, 54(9):1–40, 2021.
- Ozan Sener and Silvio Savarese. Active learning for convolutional neural networks: A core-set approach. *arXiv preprint arXiv:1708.00489*, 2017.
- Burr Settles. Active learning literature survey. 2009.
- Burr Settles. From theories to queries: Active learning in practice. In *Active learning and experimental design workshop in conjunction with AISTATS 2010*, pages 1–18. JMLR Workshop and Conference Proceedings, 2011.
- Aarohi Srivastava, Abhinav Rastogi, Abhishek Rao, Abu Awal Md Shoeb, Abubakar Abid, Adam Fisch, Adam R Brown, Adam Santoro, Aditya Gupta, Adrià Garriga-Alonso, et al. Beyond the imitation game: Quantifying and extrapolating the capabilities of language models. *arXiv preprint arXiv:2206.04615*, 2022.

- Hongjin Su, Weijia Shi, Jungo Kasai, Yizhong Wang, Yushi Hu, Mari Ostendorf, Wen-tau Yih, Noah A. Smith, Luke Zettlemoyer, and Tao Yu. One embedder, any task: Instruction-finetuned text embeddings. 2022. URL <https://arxiv.org/abs/2212.09741>.
- Mirac Suzgun, Nathan Scales, Nathanael Schärli, Sebastian Gehrmann, Yi Tay, Hyung Won Chung, Aakanksha Chowdhery, Quoc V Le, Ed H Chi, Denny Zhou, et al. Challenging big-bench tasks and whether chain-of-thought can solve them. *arXiv preprint arXiv:2210.09261*, 2022.
- Simon Tong and Daphne Koller. Support vector machine active learning with applications to text classification. *Journal of machine learning research*, 2(Nov):45–66, 2001.
- Hugo Touvron, Thibaut Lavril, Gautier Izacard, Xavier Martinet, Marie-Anne Lachaux, Timothée Lacroix, Baptiste Rozière, Naman Goyal, Eric Hambro, Faisal Azhar, et al. Llama: Open and efficient foundation language models. *arXiv preprint arXiv:2302.13971*, 2023.
- Joaquin Vanschoren, Jan N. van Rijn, Bernd Bischl, and Luis Torgo. Openml: Networked science in machine learning. *SIGKDD Explorations*, 15(2):49–60, 2013. doi: 10.1145/2641190.2641198. URL <http://doi.acm.org/10.1145/2641190.2641198>.
- Roman Vershynin. High-dimensional probability. *University of California, Irvine*, 2020.
- Andrew J Wagenmaker, Yifang Chen, Max Simchowitz, Simon Du, and Kevin Jamieson. Reward-free rl is no harder than reward-aware rl in linear markov decision processes. In *International Conference on Machine Learning*, pages 22430–22456. PMLR, 2022.
- Dan Wang and Yi Shang. A new active labeling method for deep learning. In *2014 International joint conference on neural networks (IJCNN)*, pages 112–119. IEEE, 2014.
- Xinyi Wang, Wanrong Zhu, and William Yang Wang. Large language models are implicitly topic models: Explaining and finding good demonstrations for in-context learning. *arXiv preprint arXiv:2301.11916*, 2023a.
- Yihan Wang, Jatin Chauhan, Wei Wang, and Cho-Jui Hsieh. Universality and limitations of prompt tuning. *arXiv preprint arXiv:2305.18787*, 2023b.
- Zhendong Wang, Yifan Jiang, Yadong Lu, Yelong Shen, Pengcheng He, Weizhu Chen, Zhangyang Wang, and Mingyuan Zhou. In-context learning unlocked for diffusion models. *arXiv preprint arXiv:2305.01115*, 2023c.
- Jason Wei, Maarten Bosma, Vincent Y Zhao, Kelvin Guu, Adams Wei Yu, Brian Lester, Nan Du, Andrew M Dai, and Quoc V Le. Finetuned language models are zero-shot learners. *arXiv preprint arXiv:2109.01652*, 2021.
- Yuxin Wen, Neel Jain, John Kirchenbauer, Micah Goldblum, Jonas Geiping, and Tom Goldstein. Hard prompts made easy: Gradient-based discrete optimization for prompt tuning and discovery. *arXiv preprint arXiv:2302.03668*, 2023.
- Zhiyong Wu, Yaoxiang Wang, Jiacheng Ye, and Lingpeng Kong. Self-adaptive in-context learning. *arXiv preprint arXiv:2212.10375*, 2022.
- Sang Michael Xie, Aditi Raghunathan, Percy Liang, and Tengyu Ma. An explanation of in-context learning as implicit bayesian inference. *arXiv preprint arXiv:2111.02080*, 2021.
- Junwen Yang and Vincent Tan. Minimax optimal fixed-budget best arm identification in linear bandits. In *Advances in Neural Information Processing Systems 35*, 2022.
- Shukang Yin, Chaoyou Fu, Sirui Zhao, Ke Li, Xing Sun, Tong Xu, and Enhong Chen. A survey on multimodal large language models. *arXiv preprint arXiv:2306.13549*, 2023.
- Youngjae Yu, Jiwan Chung, Heeseung Yun, Jack Hessel, JaeSung Park, Ximing Lu, Prithviraj Ammanabrolu, Rowan Zellers, Ronan Le Bras, Gunhee Kim, et al. Multimodal knowledge alignment with reinforcement learning. *arXiv preprint arXiv:2205.12630*, 2022.

Youngjae Yu, Jiwan Chung, Heeseung Yun, Jack Hessel, Jae Sung Park, Ximing Lu, Rowan Zellers, Prithviraj Ammanabrolu, Ronan Le Bras, Gunhee Kim, et al. Fusing pre-trained language models with multimodal prompts through reinforcement learning. In *Proceedings of the IEEE/CVF Conference on Computer Vision and Pattern Recognition*, pages 10845–10856, 2023.

Michelle Yuan, Hsuan-Tien Lin, and Jordan Boyd-Graber. Cold-start active learning through self-supervised language modeling. *arXiv preprint arXiv:2010.09535*, 2020.

Xueying Zhan, Qingzhong Wang, Kuan-hao Huang, Haoyi Xiong, Dejing Dou, and Antoni B Chan. A comparative survey of deep active learning. *arXiv preprint arXiv:2203.13450*, 2022.

Yiming Zhang, Shi Feng, and Chenhao Tan. Active example selection for in-context learning. *arXiv preprint arXiv:2211.04486*, 2022a.

Yuanhan Zhang, Kaiyang Zhou, and Ziwei Liu. What makes good examples for visual in-context learning? *arXiv preprint arXiv:2301.13670*, 2023.

Zhuosheng Zhang, Aston Zhang, Mu Li, and Alex Smola. Automatic chain of thought prompting in large language models. *arXiv preprint arXiv:2210.03493*, 2022b.

**Broader Impact:** We propose a framework for adaptive prompt design for Large Language Models (LLMs). Our method does not address the fundamental ethical and societal challenges inherent to these models. Specifically, it does not correct the biases or discriminatory outputs that may exist in the LLMs. Additionally, our approach does not solve the issue of LLMs generating reasonable but inaccurate information, known as hallucinations. Therefore, while our method improves the functionality of LLMs, it is essential for users and developers to use these models responsibly and remain aware of their limitations, particularly in terms of content accuracy and fairness.

## A Related Work

We study the problem of choosing human demonstrations adaptively to get the desired output from the LLM as quickly as statistically possible. We use active learning to choose them and then ask a human to label them. Finally, the human demonstrations are fed as in-context input to the LLM together with the main user query, to obtain the desired output. Thus the name is active transductive inference. Prior works on prompt-tuning and transductive inference [Lester et al., 2021, Dong et al., 2022, Zhang et al., 2022a, Min et al., 2022, Wu et al., 2022, Yu et al., 2022, Suzgun et al., 2022, Liu et al., 2023a, Yu et al., 2023, Liu et al., 2023b] focus on hard prompt-tuning where the user must carefully handcraft the prompt to get the desired output for tasks like movie recommendation, disambiguation QA, navigation, etc. Such examples of carefully handcrafting hard prompts with demonstrations can be found in Suzgun et al. [2022], Srivastava et al. [2022]. These papers also show how failing to design such prompts with demonstrations can lead the LLM to predict wrong outputs. Note that we adaptively design the prompt through carefully chosen demonstrations. In our experiments, we show significant improvement over randomly chosen demonstrations.

The problem of active learning is also related to *dataset augmentation* [Dukler et al., 2021]. In this work, the most informative unlabeled examples are chosen by optimizing the error of the model on the validation set. The gradient of the validation set error with respect to the weights of unlabeled examples has a closed form when the original model is linearized. The main difference in active learning, including in our work, is that labeling all unlabeled examples would be costly. Therefore, the labels are not available in advance and are queried adaptively. We also learn in context and do not assume that the gradient information of the LLM is available. Prompt composition has also been an active area of research. Bowman et al. [2023] proposed a-la-carte prompt tuning, where prompts are tuned on individual datasets and composed at inference time to mimic the performance of the model that would have been trained on the union of the corresponding datasets. This idea has been further extended by Perera et al. [2023], where prompts for previously unseen tasks are obtained by linearly combining prompts from known tasks. To do this, they use spectral decomposition and project prompts from known tasks to a lower dimensional space. In our work, we do not tune prompts or compose simpler models. We actively probe an LLM, treated as a black box without any extra side information, to answer a test example as accurately as possible, with as little variance in the answer as possible.

Recently there has been a lot of progress in prompt tuning (or aligning). Hassan et al. [2023] studies prompt aligning for a single test sample to adapt to multi-modal test prompts at test time by minimizing the feature distribution shift to the test domain. In contrast in this paper, we study adapting prompts for many test samples without the feature distribution shift assumption. The Wang et al. [2023a] trains a smaller LLM to select demonstrations for a larger LLM. However, we rely on active learning to select the smallest number of informative prompts to be labeled by human labelers. This avoids finetuning a smaller LLM for individual tasks. Wang et al. [2023c] studies transductive inference for diffusion models for a different setting where given a pair of task-specific example images, such as depth from/to image and scribble from/to image, and text guidance, the model automatically understands the underlying task and performs the same task on a new query image following the text guidance. However, in our setting, we do not explicitly encode any guidance text. The Wen et al. [2023] proposes to mix the nearest neighbor method with gradient optimization to select prompts during test time. Similarly, Zhang et al. [2023] proposes a nearest neighbor approach to select in-context examples for computer vision tasks. We compare our approach against such nearest-neighbor selection algorithms. Finally, Bai et al. [2023], Wang et al. [2023b] analyze transductive inference theoretically to understand its universality, generalization capability, and limitations. In contrast, we only do a theoretical analysis of AIPD to show it maximally reduces the estimated variance of the answer to the user’s query. The Zhang et al. [2022b] study the chain-of-thought prompting where they automatically select the prompt using a clustering-based approach.

There are some related works in the area of medical diagnosis chatbot examples that we shared in the introduction. One notable study Caruccio et al. [2024], although not utilizing machine learning techniques, provides valuable insights with its implementation of three hardcoded prompt designs for accurate diagnosis. These designs, however, do not engage in active learning, as they lack the capability to adapt based on user input. Similarly, Kuroiwa et al. [2023] gives more insights into self-diagnostics of orthopedic diseases using ChatGPT. In contrast, web applications such as Buoy Health BuoyHealth and Live Healthily livehealthily employ a more dynamic approach, actively

tailoring subsequent questions based on users’ responses. This aligns with active learning principles but it is not clear what techniques they apply and is notably underexplored in academic literature, indicating a potential area for further research. Our setting also goes beyond the single shot active prompt tuning studied in [Margatina et al. \[2023\]](#). Note that this work studies prompt tuning only for one iteration, and does not take into account the historical context. So it has limited ability for complex tasks like ARC [[Alford, 2021](#)] and PCFG [[Hupkes et al., 2020](#)] as well as handling vector labels like [GO](#) and [SAL](#).

**Active Learning (AL):** Recently, there has been a lot of focus on using deep [AL](#) to finetune [LLMs](#). All [AL](#) algorithms tend to balance uncertainty and diversity in the selection of unlabeled examples. We briefly discuss them below and also highlight the main difference of these approaches with prompt aligning with [GO](#) and [SAL](#).

(1) **Coreset:** This is a pure diversity-based approach using a coreset selection. In every iteration, first, the embedding of each unlabeled example is computed from the network’s penultimate layer, and then unlabeled examples are selected using a greedy furthest-first traversal conditioned on all labeled examples [[Sener and Savarese, 2017](#), [Geifman and El-Yaniv, 2017](#), [Citovsky et al., 2021](#)]. Observe that in our setting we do not have access to the penultimate layer of the [LLM](#).

(2) **Least:** This is an uncertainty-based active learning algorithm. Here, the uncertainty score of an unlabeled example is its predicted class probability. At every iteration, this algorithm then samples unlabeled examples with the smallest uncertainty scores [[Settles, 2009, 2011](#), [Wang and Shang, 2014](#)].

(3) **Margin:** This is also an uncertainty-based active learning algorithm [[Tong and Koller, 2001](#), [Balcan et al., 2009](#), [Settles, 2009](#)]. At every iteration  $t$  it selects unlabeled examples that are sorted according to their multiclass margin score and then selects unlabeled examples that are the hardest to discriminate and can be thought of as examples closest to their class margin. However, in our setting, we do not have any information on the hypothesis space of the [LLM](#) and hence cannot implement such a baseline.

(4) **Entropy:** This is also an uncertainty-based active learning algorithm [Wang and Shang \[2014\]](#), [Kremer et al. \[2014\]](#), [Diao et al. \[2023\]](#). At every iteration  $t$  it selects unlabeled examples according to the entropy of the example’s predictive class probability distribution. We show that [Greedy-NN-max-mean](#) is outperformed significantly by [GO](#) and [SAL](#) in the prediction, pcfg, or arc tasks.

(5) **Badge:** This is an algorithm that combines both uncertainty and diversity sampling [[Ash et al., 2019, 2021](#)]. For each unlabeled example  $x$  its gradient embedding  $g_x$  is computed with respect to the parameters of the model’s penultimate layer. Finally, [Badge](#) chooses a batch of samples to sample by applying  $k$ -Means++ [[Arthur and Vassilvitskii, 2006](#)] on the gradient embeddings. Again recall that we cannot implement such a baseline as we do not have access to the [LLMs](#) last layer.

(6) **Badge-KM:** This algorithm is similar to [Badge](#) but in the final step instead of  $k$ -Means++ it uses  $k$ -Means on the gradient embeddings. In [Yuan et al. \[2020\]](#) it is observed that applying  $k$ -Means on the embeddings results in an increase in accuracy over baselines in some datasets. Further [Yuan et al. \[2020\]](#) observed from the t-SNE plots that  $k$ -Means select centers that are further apart compared to the ones chosen by  $k$ -Means++ which leads to more diverse sampling in batches.

(7) **Bald:** Bayesian Active Learning by Disagreements [[Kirsch et al., 2019](#), [Gal et al., 2017](#)] chooses unlabeled examples that are expected to maximize the information gained from the model parameters  $\theta_t$ , i.e. the mutual information between predictions and model posterior.

A more comprehensive survey on how [AL](#) is used for finetuning deep models can be found in [Ren et al. \[2021\]](#), [Zhan et al. \[2022\]](#). The [Bhatt et al. \[2024\]](#) study how experimental design can be used to select prompts for finetuning a pre-trained [LLM](#). Some recent works have also focused on selecting unlabeled examples only within a task [Wei et al. \[2021\]](#), [Chen et al. \[2023\]](#), [Fifty et al. \[2021\]](#). However, these works are geared towards selecting prompts within a task for finetuning, whereas we focus on adaptive prompt design using experimental design. The work of [Perlitz et al. \[2023\]](#) also uses [AL](#) for finetuning prompts for [LLMs](#) to improve label efficiency. The [Kung et al. \[2023\]](#) proposes an [AL](#) framework for instruction tuning. However, their approach again focuses on selecting unlabeled examples inside each task and discriminating one task from another. However, they make the simplifying assumption that all unlabeled examples inside the tasks are equally informative which may inhibit the quality of the selected subset.

## B Proofs

This section contains the properties of our objective and proofs of our main claims.

### B.1 Properties of our objective

By the total variance decomposition for a linear model with observation variance  $\sigma^2$ , we get

$$\begin{aligned} \max_{k \in [K]} \text{var}[Y_{*,k} \mid \mathbf{x}_{*,k}, H_{T+1}] &= \max_{k \in [K]} \text{var}[\mathbb{E}[Y_{*,k} \mid \mathbf{x}_{*,k}, \theta_*, H_{T+1}] \mid \mathbf{x}_{*,k}, H_{T+1}] \\ &\quad + \max_{k \in [K]} \mathbb{E}[\text{var}[Y_{*,k} \mid \mathbf{x}_{*,k}, \theta_*, H_{T+1}] \mid \mathbf{x}_{*,k}, H_{T+1}] \\ &= \max_{k \in [K]} \sigma^2 \mathbf{x}_{*,k}^\top \widehat{\Sigma}_t^{-1} \mathbf{x}_{*,k} + \sigma^2. \end{aligned}$$

Therefore, the variance minimization of  $\max_{k \in [K]} Y_{*,k} \mid \mathbf{x}_{*,k}, H_{T+1}$  is a combinatorial optimization problem. It can be formulated as follows

$$S_* = \arg \min_{S \subseteq [n], |S|=T} f(S), \quad (3)$$

where the function  $f(S) = \max_{k \in [K]} \mathbf{x}_{*,k}^\top (\Sigma_0^{-1} + \sigma^{-2} \sum_{i \in S} \mathbf{x}_i \mathbf{x}_i^\top)^{-1} \mathbf{x}_{*,k}$  represents the uncertainty associated with any subset  $S$ , and  $S_*$  denotes the optimal subset of size  $T$ . If  $f(S)$  was monotone and supermodular in  $S$ , we would have  $(1-1/e)$ -optimality guarantees for [GO](#) [[Nemhauser et al., 1978](#)]. We start with proving the monotonicity of  $f(S)$ .

**Lemma 3.** *Function  $f(S)$  is monotonically decreasing.*

The claim is proved in [Appendix B.2](#). Now we state the definition of a supermodular function and show that  $f(S)$  is not supermodular.

**Definition 4** (Supermodular function). *Let  $[n]$  be a set of  $n$  elements. A function  $f : 2^{[n]} \rightarrow \mathbb{R}$  is supermodular if it satisfies the property of diminishing marginal returns. For any  $S_1 \subseteq S_2 \subseteq [n]$  and  $\mathbf{x} \notin S_2$ , we have  $f(S_1 \cup \{\mathbf{x}\}) - f(S_1) \leq f(S_2 \cup \{\mathbf{x}\}) - f(S_2)$ .*

**Lemma 5.** *The function  $f(S)$  is not supermodular.*

*Proof.* Take  $\Sigma_0 = I_d$ , fix  $K = 1$ ,  $\mathbf{x}_1 = (1/\sqrt{2}, 1/\sqrt{2})$ ,  $\mathbf{x}_2 = (0, 1)$ , and  $\mathbf{x}_* = (1, 0)$ . Then  $f(\{2\}) - f(\emptyset) = 0 < 0.035714 \approx f(\{1, 2\}) - f(\{1\})$ .  $\square$

### B.2 Proof of Lemma 3

Recall that the objective function is  $f(S) = \max_{k \in [K]} \mathbf{x}_{*,k}^\top (\Sigma_0^{-1} + \sigma^{-2} \sum_{i \in S} \mathbf{x}_i \mathbf{x}_i^\top)^{-1} \mathbf{x}_{*,k}$ . Without loss of generality, let  $\sigma^2 = 1$ . Fix any  $j \in [n] \setminus S$  and let  $S_+ = S \cup \{j\}$ . Then the objective value at  $S_+$  can be written as

$$f(S_+) = \max_{k \in [K]} \mathbf{x}_{*,k}^\top \left( \Sigma_0^{-1} + \sum_{i \in S_+} \mathbf{x}_i \mathbf{x}_i^\top \right)^{-1} \mathbf{x}_{*,k} = \max_{k \in [K]} \mathbf{x}_{*,k}^\top (\mathbf{A} + \mathbf{x}_j \mathbf{x}_j^\top)^{-1} \mathbf{x}_{*,k},$$

where  $\mathbf{A} = \Sigma_0^{-1} + \sum_{i \in S} \mathbf{x}_i \mathbf{x}_i^\top$ . By the Sherman–Morrison formula, we have

$$(\mathbf{A} + \mathbf{x}_j \mathbf{x}_j^\top)^{-1} = \mathbf{A}^{-1} - \frac{\mathbf{A}^{-1} \mathbf{x}_j \mathbf{x}_j^\top \mathbf{A}^{-1}}{1 + \mathbf{x}_j^\top \mathbf{A}^{-1} \mathbf{x}_j}.$$

Now note that  $\frac{\mathbf{A}^{-1} \mathbf{x}_j \mathbf{x}_j^\top \mathbf{A}^{-1}}{1 + \mathbf{x}_j^\top \mathbf{A}^{-1} \mathbf{x}_j}$  is a positive semi-definite matrix for any  $\mathbf{x}_j$  and any positive semi-

definite matrix  $\mathbf{A}$ . As a result,  $\mathbf{x}_{*,k}^\top \frac{\mathbf{A}^{-1} \mathbf{x}_j \mathbf{x}_j^\top \mathbf{A}^{-1}}{1 + \mathbf{x}_j^\top \mathbf{A}^{-1} \mathbf{x}_j} \mathbf{x}_{*,k} \geq 0$  holds for any  $\mathbf{x}_{*,k}$  and thus

$$f(S_+) = \max_{k \in [K]} \mathbf{x}_{*,k}^\top \mathbf{A}^{-1} \mathbf{x}_{*,k} - \mathbf{x}_{*,k}^\top \frac{\mathbf{A}^{-1} \mathbf{x}_j \mathbf{x}_j^\top \mathbf{A}^{-1}}{1 + \mathbf{x}_j^\top \mathbf{A}^{-1} \mathbf{x}_j} \mathbf{x}_{*,k} \leq \max_{k \in [K]} \mathbf{x}_{*,k}^\top \mathbf{A}^{-1} \mathbf{x}_{*,k} = f(S).$$

This proves our claim.

### B.3 Proof of Theorem 1

The proof is under the assumption that at round  $t$ , the training examples can be partitioned as  $\mathcal{X}_{\text{examples}} = S_k \cup \bar{S}_k$ . The set  $S_k$  represents examples that are close to  $\mathbf{x}_{*,k}$ . The set  $S_k$  is convex and define  $\alpha_k \geq 0$  such that  $\mathbf{x}^\top \mathbf{y} \geq \alpha_k$  for all  $\mathbf{x}, \mathbf{y} \in S_k$ . The set  $\bar{S}_k$  represents examples that are not close to  $\mathbf{x}_{*,k}$ . It is defined  $\beta_k \geq 0$  such that  $\mathbf{x}^\top \mathbf{y} \leq \beta_k$  for all  $\mathbf{x} \in S_k$  and  $\mathbf{y} \in \bar{S}_k$ . Define  $\alpha_{\min} = \min_k \alpha_k$ , and  $\beta_{\max} = \beta_{\max}$ .

Define the set  $S = \bigcap_{k=1}^K S_k$  as the set of all examples that are close to all  $\{\mathbf{x}_{*,k}\}_{k=1}^K$  and  $\bar{S} = \bigcup_{k=1}^K \bar{S}_k$  as the set of all examples that are not close to all  $\{\mathbf{x}_{*,k}\}_{k=1}^K$ . Assume  $S \neq \{\emptyset\}$  and  $|S| > T$ .

The inverse of the covariance matrix after  $t-1$  observations is

$$\widehat{\Sigma}_t^{-1} = \mathbf{\Lambda}_t = \mathbf{I}_d + \sum_{\ell=1}^{t-1} X_\ell X_\ell^\top = \sum_{i=1}^d \lambda_{t,i} \mathbf{v}_{t,i} \mathbf{v}_{t,i}^\top.$$

The latter is the eigendecomposition of  $\mathbf{\Lambda}_t$ , where  $\lambda_{t,i}$  is the  $i$ -th largest eigenvalue and  $\mathbf{v}_{t,i}$  is the corresponding eigenvector. Note that  $\mathbf{\Lambda}_t^{-1} = \sum_{i=1}^d \lambda_{t,i}^{-1} \mathbf{v}_{t,i} \mathbf{v}_{t,i}^\top$ . To simplify exposition, we assume that all examples have unit length. We analyze the eigenvalues of  $\mathbf{\Lambda}_t$  first.

**Lemma 6.** *For all  $i \in [d]$ ,  $1 \leq \lambda_{t,i} \leq t$ . Moreover, let  $X_\ell \in S$  hold for all  $\ell \in [t-1]$ . Then  $\lambda_{t,1} \geq \alpha_{\min}^2(t-1) + 1$ .*

*Proof.* The first claim follows directly from the definition of  $\mathbf{\Lambda}_t$  and that  $\|X_\ell\|_2 \leq 1$ . The second claim is proved using the definition of the maximum eigenvalue,

$$\lambda_{t,1} = \mathbf{v}_{t,1}^\top \mathbf{\Lambda}_t \mathbf{v}_{t,1} \geq \mathbf{x}_{*,k}^\top \left( \mathbf{I}_d + \sum_{\ell=1}^{t-1} X_\ell X_\ell^\top \right) \mathbf{x}_{*,k} \geq \alpha_{\min}^2(t-1) + 1.$$

The last inequality follows from  $\mathbf{x}_{*,k}^\top X_\ell \geq \alpha_{\min}$ . This completes the proof.  $\square$

We continue with claims about the eigenvectors of  $\mathbf{\Lambda}_t$ .

**Lemma 7.** *Let  $X_\ell \in S$  hold for all  $\ell \in [t-1]$ . Then  $\mathbf{v}_{t,1} \in S$ . Moreover, let  $\beta_{\max} \geq 1 - \alpha_{\min}^2$ . Then  $\mathbf{v}_{t,i} \in \bar{S}$  for all  $i \geq 2$ .*

*Proof.* Since all  $X_\ell \in S$  and  $S$  is a convex set,  $\mathbf{v}_{t,1} \in S$ . Now take any  $\mathbf{x} \in S$  and  $i \geq 2$ , and note that

$$(\mathbf{x}^\top \mathbf{v}_{t,i})^2 \leq \sum_{i=2}^d (\mathbf{x}^\top \mathbf{v}_{t,i})^2 = 1 - (\mathbf{x}^\top \mathbf{v}_{t,1})^2 \leq 1 - \alpha_{\min}^2.$$

We use that  $\sum_{i=1}^d (\mathbf{x}^\top \mathbf{v}_{t,i})^2 = 1$  and  $\mathbf{x}^\top \mathbf{v}_{t,1} \geq \alpha_{\min}$ . Therefore, when  $\beta_{\max} \geq 1 - \alpha_{\min}^2$ , we have  $\mathbf{v}_{t,i} \in \bar{S}$  for all  $i \geq 2$ .  $\square$

Our analysis has two parts. First, we bound the approximation error under the assumption that  $X_\ell \in S$  holds for all  $\ell \in [T]$ . Second, we show how to choose  $\alpha_{\min}$  and  $\beta_{\max}$  to guarantee this. We start with the approximation error.

**Lemma 8.** *Let  $X_\ell \in S$  hold for all  $\ell \in [T]$ . Then for any  $\mathbf{x}_{*,k}$*

$$\mathbf{x}_{*,k}^\top \mathbf{\Lambda}_{T+1}^{-1} \mathbf{x}_{*,k} \leq \frac{1}{\alpha_{\min}^2 T + 1} + (1 - \alpha_{\min}^2).$$

*Proof.* We start with

$$\mathbf{x}_{*,k}^\top \mathbf{\Lambda}_{T+1}^{-1} \mathbf{x}_{*,k} = \sum_{i=1}^d \lambda_{T+1,i}^{-1} \mathbf{x}_{*,k}^\top \mathbf{v}_{T+1,i} \mathbf{v}_{T+1,i}^\top \mathbf{x}_{*,k} \leq \frac{(\mathbf{x}_{*,k}^\top \mathbf{v}_{T+1,1})^2}{\alpha_{\min}^2 T + 1} + \sum_{i=2}^d (\mathbf{x}_{*,k}^\top \mathbf{v}_{T+1,i})^2.$$

The inequality uses lower bounds in Lemma 6. Then we apply  $\mathbf{x}_{*,k}^\top \mathbf{v}_{T+1,1} \leq 1$  and  $\sum_{i=2}^d (\mathbf{x}_{*,k}^\top \mathbf{v}_{T+1,i})^2 \leq 1 - \alpha_{\min}^2$ .  $\square$

Now we prove by induction that  $X_\ell \in S$  holds for all  $\ell \in [T]$ .

**Lemma 9.** *Let  $X_\ell \in S$  hold for all  $\ell \in [t-1]$ . Suppose that  $t \leq \frac{\alpha_{\min}^2}{(\beta + \sqrt{2})\beta d}$ . Then  $\mathbf{x}_t \in S$ .*

*Proof.* Our algorithm chooses an example  $\mathbf{x}_t \in S$  when for all  $\mathbf{x}_{*,k}$

$$\frac{\mathbf{x}_{*,k}^\top \Lambda_t^{-1} \mathbf{x} \mathbf{x}^\top \Lambda_t^{-1} \mathbf{x}_{*,k}}{1 + \mathbf{x}^\top \Lambda_t^{-1} \mathbf{x}} \geq \frac{\mathbf{x}_{*,k}^\top \Lambda_t^{-1} \mathbf{y} \mathbf{y}^\top \Lambda_t^{-1} \mathbf{x}_{*,k}}{1 + \mathbf{y}^\top \Lambda_t^{-1} \mathbf{y}}$$

holds for any  $\mathbf{x} \in S$  and  $\mathbf{y} \in \bar{S}$ . Since  $0 \leq \mathbf{v}^\top \Lambda_t^{-1} \mathbf{v} \leq 1$  for any  $\|\mathbf{v}\|_2 \leq 1$ , the above event occurs when

$$\min_k (\mathbf{x}_{*,k}^\top \Lambda_t^{-1} \mathbf{x})^2 = \min_k \mathbf{x}_{*,k}^\top \Lambda_t^{-1} \mathbf{x} \mathbf{x}^\top \Lambda_t^{-1} \mathbf{x}_{*,k} \geq 2 \max_{k \in [K]} \mathbf{x}_{*,k}^\top \Lambda_t^{-1} \mathbf{y} \mathbf{y}^\top \Lambda_t^{-1} \mathbf{x}_{*,k} = 2 \max_{k \in [K]} (\mathbf{x}_{*,k}^\top \Lambda_t^{-1} \mathbf{y})^2.$$

We start with an upper bound on the right-hand side,

$$\max_{k \in [K]} |\mathbf{x}_{*,k}^\top \Lambda_t^{-1} \mathbf{y}| \leq \max_{k \in [K]} \sum_{i=1}^d \lambda_{t,i}^{-1} |\mathbf{x}_{*,k}^\top \mathbf{v}_{t,i} \mathbf{v}_{t,i}^\top \mathbf{y}| \leq \beta_{\max} d.$$

Here we use  $\lambda_{t,i} \geq 1$  (Lemma 6), and that  $\mathbf{v}_{t,1}^\top \mathbf{y} \leq \beta_{\max}$  and  $\mathbf{x}_*^\top \mathbf{v}_{t,i} \leq \beta_{\max}$  when  $i \geq 2$ .

Now we bound the left-hand side as

$$\min_k |\mathbf{x}_{*,k}^\top \Lambda_t^{-1} \mathbf{x}| \geq \min_k \lambda_{t,1}^{-1} |\mathbf{x}_{*,k}^\top \mathbf{v}_{t,1} \mathbf{v}_{t,1}^\top \mathbf{x}| - \sum_{i=2}^d \lambda_{t,i}^{-1} |\mathbf{x}_{*,k}^\top \mathbf{v}_{t,i} \mathbf{v}_{t,i}^\top \mathbf{x}| \geq \frac{\alpha_{\min}^2}{t} - \beta_{\max}^2 d.$$

To bound the first term, we use  $\lambda_{t,1} \leq t$ , and that  $\mathbf{x}_*^\top \mathbf{v}_{t,1} \geq \alpha_{\min}$  and  $\mathbf{v}_{t,1}^\top \mathbf{x} \geq \alpha_{\min}$ . To bound the second term, we use  $\lambda_{t,i} \geq 1$ , and that  $\mathbf{x}_*^\top \mathbf{v}_{t,i} \leq \beta_{\max}$  and  $\mathbf{v}_{t,i}^\top \mathbf{x} \leq \beta_{\max}$ .

Now we chain all inequalities and get that our algorithm chooses an example  $\mathbf{x}_t \in S$  when

$$t \leq \frac{\alpha_{\min}^2}{(\beta_{\max} + \sqrt{2})\beta_{\max} d}.$$

This completes the proof.  $\square$

#### B.4 Proof of Theorem 2

Consider the test examples  $\{\mathbf{x}_*\}_{k=1}^K$ . Recall that  $H_t = (X_\ell, Y_\ell)_{\ell \in [t-1]}$  is the history till round  $t$ . Then the posterior variance is

$$\hat{\Sigma}_t = \left( \Sigma_0^{-1} + \sigma^{-2} \sum_{\ell=1}^{t-1} X_\ell X_\ell^\top \right)^{-1}$$

and  $\hat{\theta}_t = \hat{\Sigma}_t \left( \Sigma_0^{-1} \theta_0 + \sigma^{-2} \sum_{\ell=1}^{t-1} X_\ell Y_\ell \right)$ . Now fix a  $X_t$  at round  $t$ . Then  $Y_t = X_t^\top \theta_* + \epsilon_t$  where  $\theta_* | H_t \sim \mathcal{N}(\hat{\theta}_t, \hat{\Sigma}_t)$  and  $\epsilon_t \sim \mathcal{N}(0, \sigma^2)$ . Then  $\theta_* | H_{t+1} \sim \mathcal{N}(\hat{\theta}_{t+1}, \hat{\Sigma}_{t+1})$  holds for any  $Y_t$ .

Now fix an  $\mathbf{x}_i \in \mathcal{X}_{\text{examples}}$  and add it to  $\hat{\Sigma}_t$  such that

$$\hat{\Sigma}_{t,i} = \left( \Sigma_0^{-1} + \sigma^{-2} \left( \sum_{\ell=1}^{t-1} X_\ell X_\ell^\top + \mathbf{x}_i \mathbf{x}_i^\top \right) \right)^{-1}.$$

Define  $\hat{\sigma}_{t,i,k}^2 = \frac{1}{m} \sum_{j=1}^m (\tilde{Y}_{t,i,k}^{(j,1)} - \tilde{Y}_{t,i,k}^{(j,2)})^2$  and the  $\mathbb{E}[\hat{\sigma}_{t,i,k}^2] = \sigma_{t,i,k}^2$ . Then define  $\sigma_{t,i,\max}^2 = \max_{k \in [K]} \mathbb{E}[\hat{\sigma}_{t,i,k}^2]$ . Then using Lemma 10 we can show that with probability  $(1 - \delta)$

$$\sigma_{t,i,\max}^2 \left[ 1 - 2\sqrt{\frac{\log(1/\delta)}{m}} \right] \leq \max_{k \in [K]} \hat{\sigma}_{t,i,k}^2 \leq \sigma_{t,i,\max}^2 \left[ 1 + 2\sqrt{\frac{\log(1/\delta)}{m}} + \frac{2\log(1/\delta)}{m} \right] \quad (4)$$

Set  $m \geq 8 \log(1/\delta)$  in (4). It follows then that

$$\frac{1}{2} \sigma_{t,i,\max}^2 \leq \max_{k \in [K]} \frac{1}{m} \sum_{j=1}^m (\tilde{Y}_{t,i,k}^{(j,1)} - \tilde{Y}_{t,i,k}^{(j,2)})^2 \leq \frac{5}{2} \sigma_{t,i,\max}^2.$$

Hence, to minimize the quantity  $\max_{k \in [K]} \tilde{Y}_{t,i,k}^{(j,1)} - \tilde{Y}_{t,i,k}^{(j,2)}$  we should be minimizing the variance  $2 \max_{k \in [K]} \mathbf{x}_{*,k}^\top \hat{\Sigma}_{t,i} \mathbf{x}_{*,k} + \sigma^2$ . Observe that minimizing the variance in SAL leads to minimizing the quantity  $2 \max_{k \in [K]} \mathbf{x}_{*,k}^\top \hat{\Sigma}_{t,i} \mathbf{x}_{*,k} + \sigma^2$  which is same as minimizing the score  $\max_{k \in [K]} \mathbf{x}_{*,k}^\top \hat{\Sigma}_{t,i} \mathbf{x}_{*,k}$  for GO. The claim of the theorem follows.

**Lemma 10.** Fix round  $t \in [T]$ , a sample example  $\mathbf{x}_i$ , and a test example  $\mathbf{x}_{*,k}$ , and failure probability  $\delta \in (0, 1)$ . Suppose that  $m > 4 \log(1/\delta)$ . Define  $\hat{\sigma}_{t,i,k}^2 = \frac{1}{m} \sum_{j=1}^m (\tilde{Y}_{t,i,k}^{(j,1)} - \tilde{Y}_{t,i,k}^{(j,2)})^2$  and the  $\mathbb{E}[\hat{\sigma}_{t,i,k}^2] = \sigma_{i,k}^2$ . Then

$$\mathbb{P} \left( \hat{\sigma}_{t,i,k}^2 \leq \sigma_{i,k}^2 \left[ 1 - 2 \sqrt{\frac{\log(1/\delta)}{m}} \right] \right) \leq \delta$$

holds with probability at least  $1 - \delta$ . Analogously,

$$\mathbb{P} \left( \hat{\sigma}_{t,i,k}^2 \geq \sigma_{i,k}^2 \left[ 1 + 2 \sqrt{\frac{\log(1/\delta)}{m}} + \frac{2 \log(1/\delta)}{m} \right] \right) \leq \delta$$

holds with probability at least  $1 - \delta$ .

*Proof.* Fix an  $\mathbf{x}_i \in \mathcal{X}_{\text{examples}}$  and add it to  $\hat{\Sigma}_t$ . Denote this new co-variance matrix as  $\hat{\Sigma}_{t,i}$  such that

$$\hat{\Sigma}_{t,i} = \left( \Sigma_0^{-1} + \sigma^{-2} \left( \sum_{\ell=1}^{t-1} X_\ell X_\ell^\top + \mathbf{x}_i \mathbf{x}_i^\top \right) \right)^{-1}.$$

Let  $\tilde{Y}_{t,i,j}^{(1)} = \mathbf{x}_{*,k}^\top \boldsymbol{\theta}_* + \epsilon_{t,i,j,1}$ , where  $\boldsymbol{\theta}_* \mid H_t \sim \mathcal{N}(\hat{\boldsymbol{\theta}}_t, \hat{\Sigma}_{t+1})$  and  $\epsilon_{t,i,j,1} \sim \mathcal{N}(0, \sigma^2)$ . This yields that  $\tilde{Y}_{t,i,j}^{(1)} \sim \mathcal{N}(\mathbf{x}_{*,k}^\top \hat{\boldsymbol{\theta}}_{t+1}, \mathbf{x}_{*,k}^\top \hat{\Sigma}_{t,i} \mathbf{x}_{*,k} + \sigma^2)$ . Similarly  $\tilde{Y}_{t,i,j}^{(2)} = \mathbf{x}_{*,k}^\top \boldsymbol{\theta}_* + \epsilon_{t,i,j,2}$ , where  $\boldsymbol{\theta}_* \mid H_t \sim \mathcal{N}(\hat{\boldsymbol{\theta}}_{t+1}, \hat{\Sigma}_{t,i})$  and  $\epsilon_{t,i,j,2} \sim \mathcal{N}(0, \sigma^2)$ . Therefore, we get that

$$\tilde{Y}_{t,i,k}^{(j,1)} - \tilde{Y}_{t,i,k}^{(j,2)} \sim \mathcal{N}(0, 2 \mathbf{x}_{*,k}^\top \hat{\Sigma}_{t,i} \mathbf{x}_{*,k} + \sigma^2).$$

Now we proceed the same way as in Lemma 2 of Lalitha et al. [2023]. Using Cochran's theorem, we have that  $\hat{\sigma}_{t,i,k}^2 m / \sigma_{i,k}^2$  is a  $\chi^2$  random variable with  $m$  degrees of freedom. Then using (4.4) and Lemma 1 of Laurent and Massart [2000] we can show that

$$\mathbb{P} \left( m - \frac{\hat{\sigma}_{t,i,k}^2 m}{\sigma_{i,k}^2} \geq 2 \sqrt{m \log(1/\delta)} \right) \leq \delta \quad (5)$$

Dividing both sides of (5) in the probability by  $m$ , and multiplying by  $\sigma_{i,k}^2$ , we can get the following

$$\mathbb{P} \left( \sigma_{i,k}^2 (1 - 2 \sqrt{\log(1/\delta)/m}) \geq \hat{\sigma}_{t,i,k}^2 \right) \leq \delta.$$

Observe that  $1 - 2 \sqrt{\log(1/\delta)/m} > 0$ , we can divide both sides by it and get the first claim of the lemma. The second claim is proved by (4.3) in Laurent and Massart [2000], an immediate corollary of their Lemma 1, we have

$$\mathbb{P} \left( \frac{\hat{\sigma}_{t,i,k}^2 m}{\sigma_{i,k}^2} - m \geq 2 \sqrt{m \log(1/\delta)} + 2 \log(1/\delta) \right) \leq \delta$$

The claim of the lemma follows.  $\square$

## C Additional Experiments and Results

We use NVIDIA GeForce RTX 3090 GPU with 24GB RAM to load the Large Language Models for inference. The Mistral-7B model requires less than 16GB RAM, and Vinuna-13B model requires less than 22 GB RAM during execution. To run Falcon-40B model we use AWS ml-g5.12xlarge machine. To run the full set of experiments it takes 24-27 hours of compute job. We now briefly discuss the various datasets used in this work.

### C.1 Datasets

We now briefly describe the datasets used for our experiments. All the real-life datasets are from UCI [Markelle Kelly, 1988] and OpenML [Vanschoren et al., 2013] repositories. We use 4 classification and 3 regression datasets from UCI and OpenML. Additionally, we use 2 custom datasets for movie names and entity names for classification task in our experiments. These are as follows:

(1) *Iris*: We use this UCI dataset for classification task. This dataset consists of four features of flowers and three classes of flowers. We use all four features in the prompts as well as estimating the score for selecting the next action. The dataset consists of 150 instances. We randomly choose  $K = 20$  as test examples and the remaining instances as training examples.

(2) *Banknote-authentication*: We use this OpenML dataset for classification task. This dataset consists of five features of banknotes and two classes for identifying fake or original banknote. Out of these five features, we use four features in the prompts as well as estimating the score for selecting the next action. The dataset consists of 150 instances. We randomly choose  $K = 20$  as test examples and the remaining instances as training examples.

(3) *Balance-scale*: We use this OpenML dataset for classification task. This dataset consists of five features of a scale and three classes of whether the scale tips left/right or is balanced. Out of these five features, we use four features in the prompts as well as estimating the score for selecting the next action. The dataset consists of 625 instances. We randomly choose  $K = 20$  as test examples and the remaining instances as training examples.

(4) *Thyroid-new*: We use this OpenML dataset for classification task. This dataset consists of six features for thyroids and three classes. Out of these six features, we use five features in the prompts as well as estimating the score for selecting the next action. The dataset consists of 215 instances. We randomly choose  $K = 20$  as test examples and the remaining instances as training examples.

(5) *Movie-name*: We use this custom dataset for classification task. This dataset consists of movie names across five genres (classes) romance, horror, thriller, sport, and action. We convert the movie names into 768 dimensional feature embeddings using Instructor embeddings. Note that in the prompt to the LLM we only pass the movie names and the goal is to identify the common genre. The dataset consists of 100 instances. We randomly choose  $K = 20$  as test examples and the remaining instances as training examples.

(6) *Movie-theme*: We use this custom dataset for classification tasks in identifying a common theme between pairs of movies. This dataset consists of movie names across five themes (classes) good-vs-evil, man-vs-nature, redemption, Love conquers all, and coming-of-age. We convert the movie names into 768 dimensional feature embeddings using Instructor embeddings. Note that in the prompt to the LLM we only pass the pair of movie names and the goal is to identify the common theme. The dataset consists of 100 instances. We randomly choose  $K = 20$  as test examples and the remaining instances as training examples.

(7) *Entity-name*: We use this custom dataset for classification task. This dataset consists of entity names across five entity types (classes) like mountains, seas, rivers, vehicles, and celebrities. Again, we convert the entity names into 768 dimensional feature embeddings using Instructor embeddings. Note that in the prompt to the LLM we only pass the entity names and the goal is to identify the entity type. The dataset consists of 100 pairs of instances. We randomly choose  $K = 20$  pairs as test examples and the remaining instances as training examples.

(8) *Fifa*: We use this OpenML dataset for the regression task. This dataset consists of six features of players and the clubs they joined as targets. Out of these six features, we use five features in the prompts as well as estimating the score for selecting the next action. The dataset consists of

18063 instances. We randomly choose  $K = 20$  test examples and another 200 examples as training examples.

**(9) Machine-cpu:** We use this OpenML dataset for regression tasks. This dataset consists of seven features of machine cpu and the target variable is the performance of the cpu. Out of these seven features, we use five features in the prompts as well as estimating the score for selecting the next action. The dataset consists of 209 instances. We randomly choose  $K = 20$  test examples and the remaining examples as training examples.

### C.1.1 ARC Experiment

In the recent works of [Mirchandani et al. \[2023\]](#), [Srivastava et al. \[2022\]](#) they showed that LLMs behave as general pattern-matching machine. In fact they showed that LLMs can be used to solve tasks from Abstract Reasoning Corpus (ARC) tasks. In the following experiments, we choose two such tasks: (1) ARC expansion and contraction experiment and (2) ARC rotation experiment.

**(1) ARC expansion and contraction experiment:** In the expansion and contraction experiment, there are two sets of matrices of dimension  $4 \times 4$  which constitute half the examples of the feature space  $\mathcal{X}$ . The first set of input matrices have integer values in their center  $2 \times 2$  cells while all the other cells are 0. The label space  $\mathcal{Y}$  of this  $4 \times 4$  matrix is also a  $4 \times 4$  matrix where the 4 inner cells have moved to the 4 corners. These matrices are termed as expansion matrices.

Similarly, the other set of  $4 \times 4$  matrices have the 4 non-zeros values in their corners. These constitute the remaining examples in  $\mathcal{X}$ . Then the label space  $\mathcal{Y}$  is given by  $4 \times 4$  matrix where the four non-zeros cells come to the center and all the other cell values are 0. These matrices are termed as contraction matrices. This is shown in Figure 1(a).

Therefore, the feature space  $\mathcal{X}$  consists of both the expansion and contraction matrices. At every trial,  $n$  training examples and  $K$  test examples are chosen randomly from  $\mathcal{X}$ . Then we run all baselines for  $T$  iterations where the classification accuracy is calculated if the LLM is able to predict the exact matching. This experiment is shown in Table 3.

**(2) ARC rotation experiment:** In the rotation experiment, there are again two sets of matrices of dimension  $4 \times 4$  which constitute half the examples of the feature space  $\mathcal{X}$ . The first set of matrices are have integer values in their four corner cells while all the other cells are 0. The label space  $\mathcal{Y}$  of this  $4 \times 4$  matrix is also a  $4 \times 4$  matrix where the 4 corner cell values have moved  $90^\circ$  in the clockwise direction. These matrices are termed as clockwise matrices.

Similarly, the other set of  $4 \times 4$  matrices have the 4 non-zeros values in their corners. These constitute the remaining examples in the feature space  $\mathcal{X}$ . Then the label space  $\mathcal{Y}$  is given by  $4 \times 4$  matrix where the four non-zeros cells have moved  $15^\circ$  in the anti-clockwise direction and all the other cell values are 0. These matrices are termed as anti-clockwise matrices. This is shown in Figure 1(b).

Therefore, the feature space  $\mathcal{X}$  consists of both the clockwise and anti-clockwise matrices. At every trial,  $n$  training examples and  $K$  test examples are chosen randomly. Then we run all the baselines for  $T$  iterations where the classification accuracy is calculated if the LLM is able to predict the exact matching. This experiment is shown in Table 3.

### C.1.2 PCFG Experiment

In this experiment the goal is to predict the next output of a sequence. In the following experiments we choose two such tasks: (1) PCFG add-subtract experiment and (2) PCFG repeat experiment.

**(1) PCFG add-subtract experiment:** In the add-subtract experiment, there are two sets of sequence of 4 integers. The first set of sequence of 4 integers consists of odd integer values which constitute half the examples in the feature space  $\mathcal{X}$ . The label space  $\mathcal{Y}$  of this sequence of 4 odd examples is sequences of 5 integers where the last integer is added to the original sequence by adding one to the last odd integer. These sequences are termed as add examples.

Similarly, the other set of examples consists of a sequence of 4 even integer values which constitute the remaining examples in the feature space  $\mathcal{X}$ . The label space  $\mathcal{Y}$  of this sequence of 4 even integer examples is a sequence of 5 integers where the last integer is added to the original sequence by subtracting one from the last even integer. These examples are termed as even examples. This is shown in Figure 2(a).

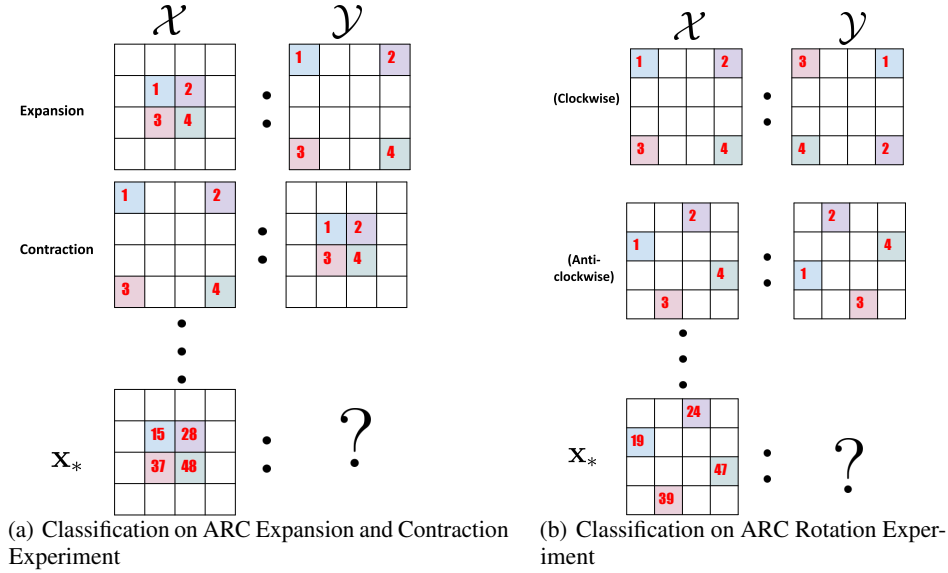


Figure 1: Explanation of ARC tasks

Therefore, the feature space  $\mathcal{X}$  consists of both the odd and even sequence of 4 integer value examples. At every trial,  $n$  training and  $K$  test examples are chosen randomly. Then we run all the baselines for  $T$  iterations where the classification accuracy is calculated if the LLM is able to predict the exact matching. This experiment is shown in Table 3.

**(2) PCFG repeat experiment:** In the repeat experiment, there are two sets of sequence of 4 integers. The first set of sequence of 4 odd integer values constitute half the examples of the feature space  $\mathcal{X}$ . The label space  $\mathcal{Y}$  of this sequence of 4 integers examples is a sequence of 5 integers where the last integer is padded to the original sequence by repeating the first odd integer. These sequences are termed as odd-repeat examples.

Similarly, the other set of examples consists of sequence of 4 even integer values which constitute the remaining examples in the feature space  $\mathcal{X}$ . The label space  $\mathcal{Y}$  of these sequence of 4 integer value examples is a sequence of 5 integers where the last integer is padded to the original sequence by repeating the second even integer. These examples are termed as even-repeat examples. This is shown in Figure 2(b).

Therefore, the feature space  $\mathcal{X}$  consist of both the odd-repeat and even-repeat examples. At every trial,  $n$  training examples and  $K$  test examples are chosen randomly. Then we run all the baselines for  $T$  iterations where the classification accuracy is calculated if the LLM is able to predict the exact matching. This experiment is shown in Table 3.

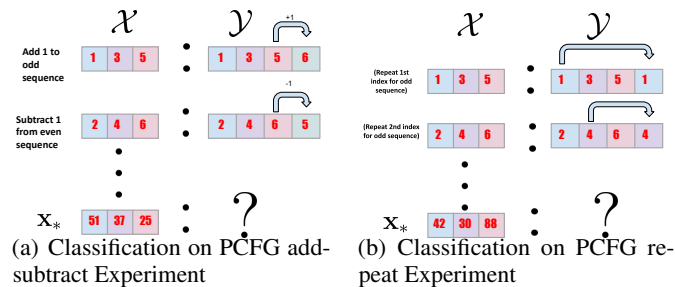


Figure 2: Explanation of PCFG task.

## D Prompt Examples

**Classification Dataset Prompts :** Below we give an example of how we use the prompts to be used in the LLM for the Iris misclassification task. Similar types of prompts can be found in Dinh et al. [2022], Suzgun et al. [2022]. This is shown in Figure 3(a). Note that since we have the feature representation of the training and test examples from the dataset, we directly use them as  $\mathbf{x}_i$  and  $\mathbf{x}_{*,k}$ .

**Regression Dataset Prompts :** In Figure 3(b) we give an example of a prompt for regression task in Fifa dataset. Note that since we have the feature representation of the training and test examples from the dataset, we directly use them as  $\mathbf{x}_i$  and  $\mathbf{x}_{*,k}$ .

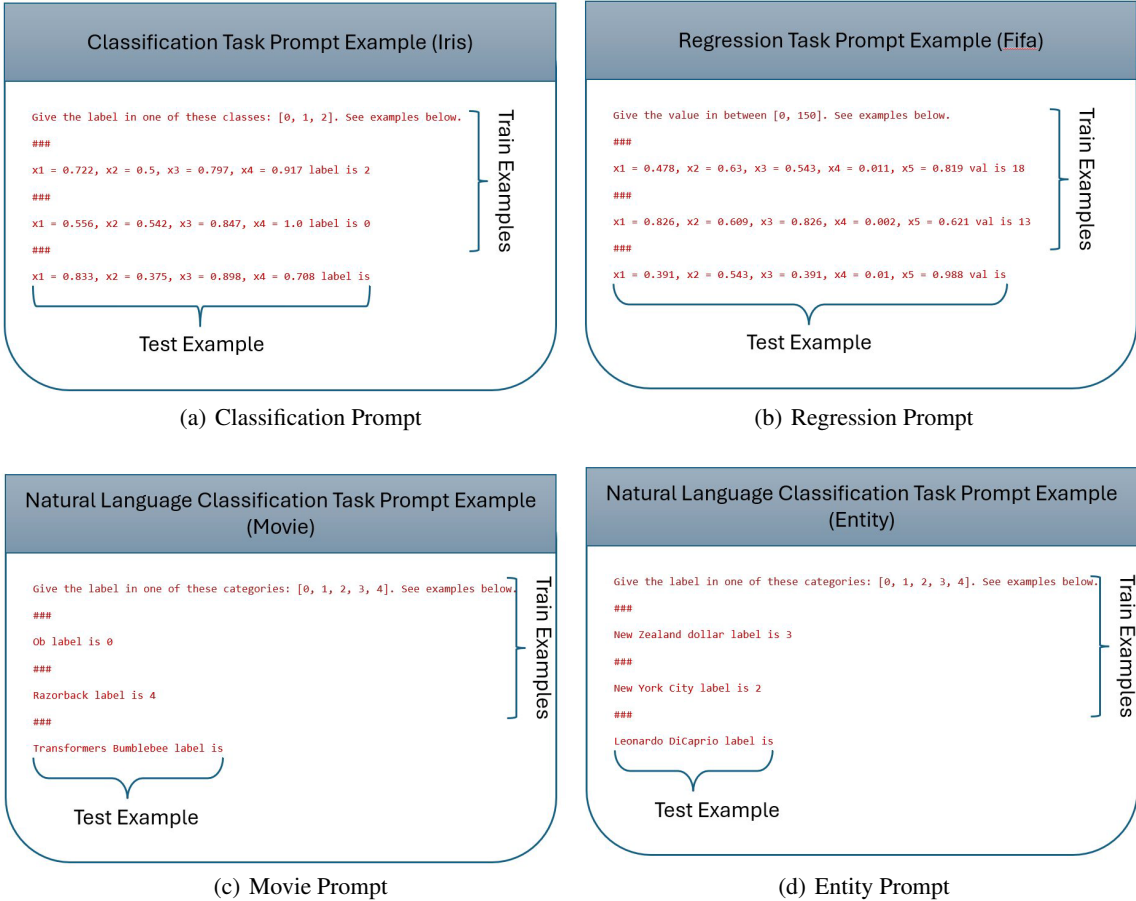


Figure 3: Prompt examples for Classification, Regression, Movie, and Prompt

**Movie Theme Experiment:** We use a similar technique as in Iris dataset for this setting. The labels of the pairs of movies belong to 5 classes as follows: good-vs-evil, man-vs-nature, redemption, Love conquers all, and coming-of-age. At every iteration, we pass  $K$  pairs of movie test examples where each  $\mathbf{x}_{*,k}$  is a pair of movies. In the example below we have  $\mathbf{x}_{*,1} = [\text{'Swallows and Amazon (2016), Grizzly (1976)'}]$ . Note that we feed the natural language text to the LLM as prompts as shown in Figure 4(a). However, to run GO, SAL, and other baselines we require a featurization of these natural language prompts. We obtain a 768 dimensional featurized representation of the pairs of movies 'Monsters Inc, Frozen (2013)' using Instructor embedding [Su et al., 2022]. This constitutes  $\mathbf{x}_i \in \mathbb{R}^{768}$  and  $\mathbf{x}_{*,k} \in \mathbb{R}^{768}$ .

**Movie Name Experiment:** We use a similar technique as in Iris dataset for this setting. The labels of the movie genres belong to 5 classes as follows: romance, horror, thriller, sport, and action. At every iteration we pass a set of test movie name examples where each  $\mathbf{x}_{*,k}$  is now movie name. Note that we feed the natural language text to the LLM as prompts as shown in Figure 3(c). However, to run GO, SAL, and other baselines we require a featurization of these natural language prompts. We

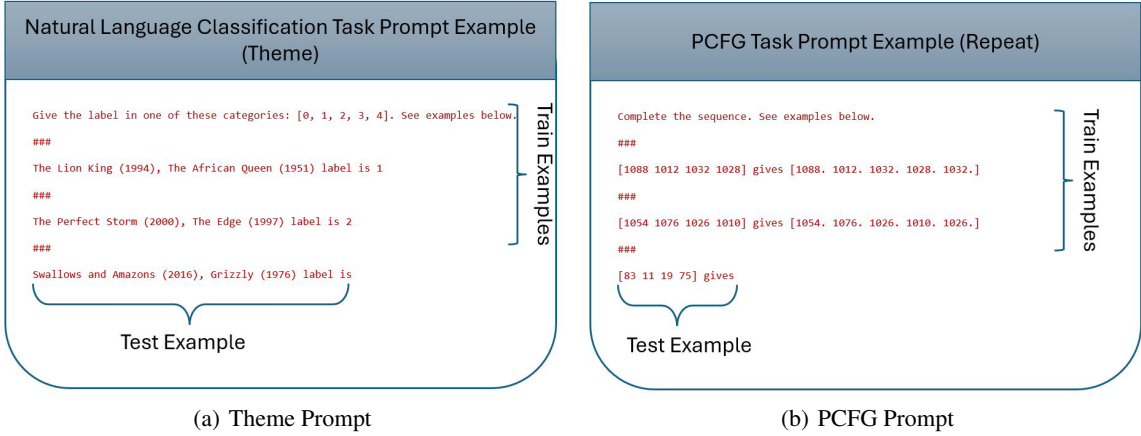


Figure 4: Prompt examples for Theme and PCFG tasks

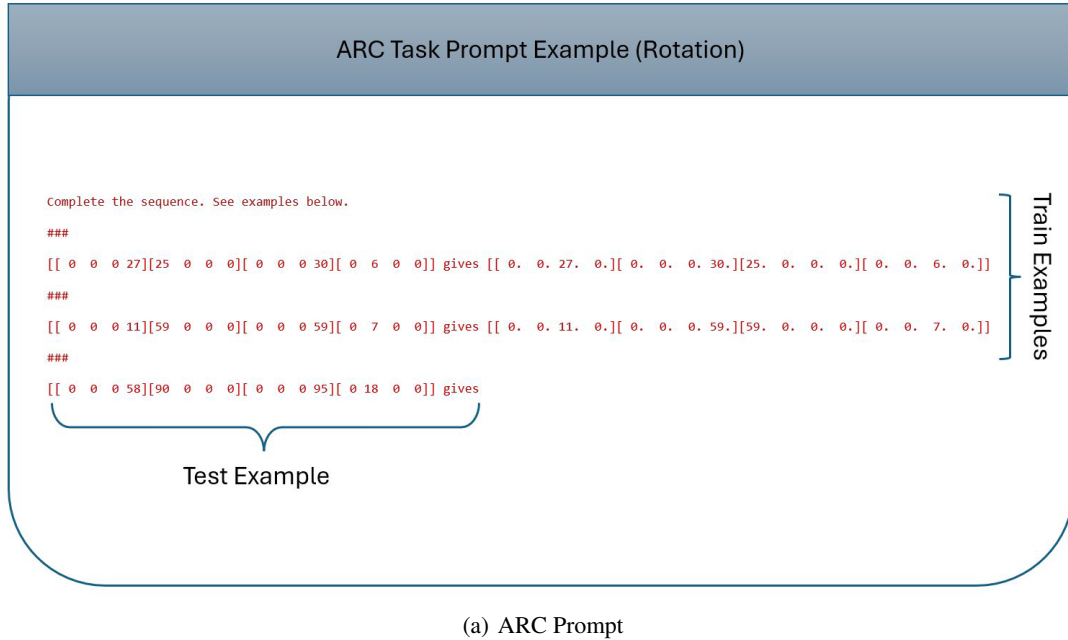


Figure 5: Prompt examples for ARC task

obtain a 768 dimensional featurized representation of the movie names using Instructor embedding [Su et al., 2022]. This constitutes  $\mathbf{x}_i \in \mathbb{R}^{768}$  and  $\mathbf{x}_{*,k} \in \mathbb{R}^{768}$ .

**Entity Name Experiment:** The labels of the entity genres belong to 5 classes as follows: mountains, seas, rivers, vehicles, and celebrities. At every iteration, we pass a set of test entity name examples where each  $\mathbf{x}_{*,k}$  is now an entity name. Note that we feed the natural language text to the LLM as prompts as shown in Figure 3(d). However, to run GO, SAL, and other baselines we require a featurization of these natural language prompts. Again, we obtain a 768 dimensional featurized representation of the entity names using Instructor embedding [Su et al., 2022]. This constitutes  $\mathbf{x}_i \in \mathbb{R}^{768}$  and  $\mathbf{x}_{*,k} \in \mathbb{R}^{768}$ .

**PCFG Experiment:** We show an example of this prompt in Figure 4(b). Here we concatenate the sequence to obtain training examples  $\mathbf{x}_i$  and test examples  $\mathbf{x}_{*,k}$ . So a sequence of 4 integers of length 4 will be represented by  $\mathbf{x}_i, \mathbf{x}_{*,k} \in \mathbb{R}^{16}$ . Similarly the label  $Y_i$  and  $Y_{*,k}$  consist of sequence of 5 integers of length 4 which we concatenate to get a vector of length  $\mathbb{R}^{20}$ .

**ARC Experiment:** We show an example of this prompt in Figure 5(a). Here we vectorized the  $4 \times 4$  matrix to obtain training examples  $\mathbf{x}_i \in \mathbb{R}^{16}$  and test examples  $\mathbf{x}_{*,k} \in \mathbb{R}^{16}$ . Similarly the label  $Y_i$  and  $Y_{*,k}$  consist of vectorized matrices of length  $\mathbb{R}^{16}$ .

## E Table of Notations

Notations	Definition
$n$	Total unlabeled examples
$d$	Dimension of the feature
$\mathcal{X}$	Feature set
$\mathcal{Y}$	Label space
$\boldsymbol{\theta}_*$	Unknown model parameter
$\mathbf{x}_i$	Feature of sample example $i$
$\mathbf{x}_{*,k}$	$k$ -th test example
$f(\mathbf{x}, \boldsymbol{\theta}_*)$	Model
$Y_*$	Label
$H_t = (X_\ell, Y_\ell)_{\ell \in [t-1]}$	History of $t - 1$ previously labeled examples
$p(\cdot   \mathbf{x}, H_t)$	Distribution of the label of example $\mathbf{x}$ conditioned on $H_t$
$\boldsymbol{\theta}_0$	Prior mean of the unknown model parameter $\boldsymbol{\theta}_*$
$\boldsymbol{\Sigma}_0$	Prior mean of the unknown model parameter $\boldsymbol{\theta}_*$
$\hat{\boldsymbol{\Sigma}}_t = \left( \boldsymbol{\Sigma}_0^{-1} + \sigma^{-2} \sum_{\ell=1}^{t-1} X_\ell X_\ell^\top \right)^{-1}$	Posterior covariance
$\mathcal{L}_t$	Set of labeled examples
$\mathcal{U}_t$	Set of unlabeled examples
$\hat{\boldsymbol{\theta}}_{t,i,j}$	Posterior mean

Table 5: Table of Notations